Department of Electrical and Computer Engineering

On-Line Optimal Charging Coordination of Plug-In Electric Vehicles in Smart Grid Environment

Somayeh Hajforoosh

This Thesis is presented for the Degree of
Doctor of Philosophy
of
Curtin University

March 2019

DECLARATIONS

According to my research and knowledge, there is no content previously published, in any format by anyone, except where references have been provided.

There is no material in this thesis, which has been approved, for an award of a degree or certificate anywhere.

Signature: *Somayeh Hajforoosh*

Date: 15/11/2018

ABSTRACT

Alternative pollution-free transportation technologies, including Plug-in Electric Vehicles (PEVs), their applications and performance in emerging smart grids, are becoming more popular. However, these relatively new electrical loads, with random plug-in time, location and charging rates, could have detrimental impacts on overloading of transformer and congestion in transmission lines.

In this proposed solution to PEV charging coordination and considering the importance of customer satisfaction, some vehicle owners can submit requested plug-out times, along with an associated requested State Of Charges (SOC_{Req}). Meeting these requirements is not a big problem when all of the vehicles plug-out, at their requested departure times. However, when unscheduled PEV departures occur, conventional schemes may not be able to provide acceptable levels of satisfaction amongst users. This problem can be resolved by using variable charging rates, as a strategy to adapt the power drawn by a charger from the grid to a load, in order to fully exploit grid capability and provide a high degree of user satisfaction.

In the research conducted, an Online Coordinated Charging Genetic Algorithm (OL-CC-GA), using fixed charging in smart grid (SG) has been applied. The proposed method can also perform delayed (e.g., partial-overnight or full-overnight) vehicle charging, by reducing the distribution transformer loading, with uncoordinated and coordinated PEV charging activities.

The Discrete Particle Swarm Optimization (DPSO) for PEV charging coordination, that considers residential distribution transformer life, has also been designed, coded and implemented.

In addition, two more individual algorithms, referred to as the Fuzzy Genetic Algorithm (FGA) and Fuzzy Discrete Particle Swarm Optimisation (FDPSO), have been implemented, to reduce the costs related to the system losses and generated energy. The delivered power to PEVs, is also

maximised in the optimisation process, taking into account, the loading limits of the distribution transformer, the voltage boundaries, the State Of Charges (SOCs) for each battery at the start time (initial SOC) and the final SOC.

Furthermore, this research proposes a new objective function, for the optimal on-line PEV charging coordination, taking into consideration the variable charge rates, generation costs and customer preferences. A newly enhanced on-line, coordinated method of charging, using Coordinated Aggregated Particle Swarm Optimisation (OLCC-CAPSO), has been utilized to reach the PEV charging coordination objective within the associated constraints. The objective function provides an opportunity for all PEVs to start charging as quickly as possible, whilst the customer satisfaction function is optimised, subject to network criteria, including voltage profiles, generator and distribution transformer ratings.

In this research, two different test systems, including 19-node (one of the branches of the second test system) and 449-node test systems, were used to examine the proposed algorithms, where the 449-node test system, is based on a standard 23 kV IEEE 31-node distribution test system. This test system is a combination of 22×19 residential low voltage 415 V networks, which is dedicated to PEVs.

ACKNOWLEDGMENTS

It is my great pleasure to acknowledge my supervisor, Professor Syed Islam, for his valuable advice and guidance in this study.

I would also like to thank my co-supervisor, Professor Mohammad A.S. Masoum, who supported and kindly advised me from early study to the latest point of my PhD to deeply understand the topic and develop my project.

Finally, I would like to express my special thanks to my family for their support, love and encouragement, during my research at Curtin University.

List of published papers from this thesis

[1] S. Hajforoosh, M.A.S. Masoum, S.M. Islam, "Online Optimal Variable Charge-rate Coordination of Plug-In Electric Vehicles to Maximize Customer Satisfaction and Improve Grid Performance", Electric Power Systems Research, pp.407-420, 2016.

[2] S. Hajforoosh, M.A.S. Masoum, S.M. Islam, "Real-time Charging Coordination of Plug-In Electric Vehicles based on Hybrid Fuzzy Discrete Particle Swarm Optimization", Electric Power Systems Research, pp.19-29, 2015.

[3] S. Hajforoosh, M.A.S. Masoum, S.M. Islam, "Performance Analysis of Optimal Online and Delayed Charging of Plug-in Electric Vehicles", Conference on Electrical and Electronics Engineering, 2015.

NOTATION

Index:

i,j	Counters
m	Node number
n	Total number of nodes

Parameters:

T_i	Set of particles j with better achievements than the set of particles i
P_i	Best position of the set of particle i
$S_i(t), S_j(t)$	Positions of the sets of particles i and j
Nr	Selected number of the search intervals
$f(S_i)$	The achievement of particle-i
$f(S_j)$	The better achievement by particle-j
Nit_max	The maximum number of iterations
Nit	The current number of iterations
W_{max}, W_{min}	The upper and lower limits of the inertia weighting factor
$SOC_{initial}(i)$	State of charge of the ith PEV at plug-in time (%)
$SOC_{Req}(i)$	Requested SOC of the ith PEV (%)
$N_{PEV}(\Delta t_k)$	Number of available PEVs for current time slot
$T_{Req}(i)$	Plug-out time of the ith PEV (hour)
$Bid(\Delta t_k, i)$	The price that the ith PEV owner is willing to pay at current time slot ($/kWh)
$Bid_{max}(\Delta t_k)$	Maximum offered bid by all existing PEVs at current time slot ($/kWh)
$R_{m,m+1}$	Resistance of the line segment between nodes m and $m+1$ (ohm)
$Y_{m,m+1}$	Admittance of the line segment between nodes m and $m+1$ (ohm)
$V_{oc,i}$	Open circuit voltage for i^{th} node (V)
R_i	Battery equivalent internal resistance for the ith node (ohm)
I_i^{Rated}	Rated charger current for the ith PEV (A)
Q_i	Rated battery ampere hour for the ith PEV (Ah)
CR_i^{max}	Maximum charging rate for the ith PEV (A)
$\eta_{ch}(CR_i^{best}(\Delta t_k))$	Charger efficiency for the ith PEV at the best charge-rate (%))
V_{min} and V_{max}	Lower and upper node voltage limits (per unit; p.u.)
$D_{max}(\Delta t_k)$	Maximum demand level that would normally occur without any PEVs during a day where selected to be 0.84 MW corresponding to the maximum load for the selected *DLC* (MW)
C	Ratio of charging or discharging current in A to the capacity of battery in Ah
L_j	Trip path for j^{th} PEV (km)
L_i^{max}	Rated length path that each type of PEVs can trip (km)

α_D, α_{Vl} and α_{V2}	Coefficients used to adjust the slopes of the penalty functions
k_1, k_2, k_3	Coefficients used to adjust the objective function based on the priority
$SOC(\Delta t_k, i)$	State of charge of the ith PEV at k^{th} time slot (%)
$Dt(\Delta t_k)$	Total load at current time slot (MW)
$DL(\Delta t_k)$	Daily load at current time slot (MW)
SOC_{max}	The state of charge of each battery
$P_{Load}(\Delta t_k)$	Base-load power at current time slot (MW)
θ_a	The ambient temperature in [^{0}C]
g_r	The gradient of the average winding temperature to average oil temperature at full load current

Variables:

$F_V(\Delta t_k)$	Penalty function for node voltage at current time slot
$F_D(\Delta t_k)$	Penalty function for demand (distribution transformer loading) at current time slot
$T_{Remain}(\Delta t_k, i)$	The remaining available time for charging the ith PEV at current time slot (hour)
$C_S(\Delta t_k, i)$	Customer satisfaction level for current time slot at i^{th} node (%)
$C_S(\Delta t_{k+1}, i)$	Customer satisfaction level for next time slot at i^{th} node (%)
V_i	Terminal voltage for i^{th} node (per unit; p.u.)
$I(\Delta t_k, i)$	Charging current for the ith PEV at current time slot (A)
$CR_i^{best}(\Delta t_k)$	Optimised charging rate for the ith PEV at current time slot (A)
$P_{PEV,i}(\Delta t_k)$	Consumed power for the ith PEV (KW)
$F_{cost-loss}(\Delta t_k)$	Total cost of system losses
$F_{cost-gen}(\Delta t_k)$	Cost of generation
$w_i(\Delta t_k)$	The weighting factor
$X_{pt,j}^{it}$	The position of the particle pt in the current generation for each generation
$\rho_{pt,j}^{it+1}$	A random number between 0 and 1 for each generation
$pbest_{pt,j}$	The best point found by particle pt in its past life up to the current generation
$gbest_j$	The best overall point found by the swarm of particles in their past life
$V_{pt,j}^{it}$	The agent's choice tendency
P_R	The total loss at rated load in [W] for each generation
$\Delta\theta_{o,r}$	The top-oil temperature rise at rated load in [K] for each generation
$\Delta\theta_o$	The top-oil temperature rise in [K] for each generation
F_{AA}	The transformer aging acceleration
F_{EQA}	The transformer equivalent aging
$rand_1, rand_2$	The positive random numbers generated from a uniform distribution

ACRONYMS

ADC	Analogue to Digital Converter
CAPSO	Coordinated Aggregated Particle Swarm Optimization
DLC	Daily load Curve
DPSO	Discrete Particle Swarm Optimization
EV	Electric Vehicle
FCC	Fixed Charge-rate Coordination
FDPSO	Fuzzy Discrete Particle Swarm Optimization
FES	Fuzzy Expert System
FGA	Fuzzy Genetic Algorithm
GA	Genetic Algorithm
HST	Hot Spot Temperature
LOL	Loss of Life
LP	Linear Programming
LV	Low Voltage
MEP	Market Energy Price
MSS	Maximum Sensitivity Selection
OLCC	Online Charging Coordination
OL-CC-GA	Online Charging Coordination - Genetic Algorithm
PEV	Plug-in Electric vehicle
PHEV	Plug-in Hybrid Electric Vehicle
PSO	Particle Swarm Optimization
SG	Smart Grid
SOC	State of Charge
V2G	Vehicle to Grid
VCC	Variable Charge-rate Coordination

TABLE OF CONTENTS

CHAPTER FOUR: PEV Battery Fixed and Variable Charging Scheduling in Smart Grid Using Coordinated Aggregated Particle Swarm Optimisation Considering Customer Satisfaction………...66

LIST OF FIGURES

14

LIST OF TABLES

CHAPTER ONE

INTRODUCTION

1.1. Motivations and aims

Plug-in Electric Vehicles (PEVs) are growing rapidly in popularity and interest. The PEVs' Batteries should be charged using different methods [1-6]. Those PEVs that are connected to a home or car park outlet will have charged their battery by power from the grid. If there is an extra load, there may be impacts on the distribution system, including overloading, transformer current limits and power losses. If PEV charging remains uncoordinated, then local grid problems may occur [7-11]. In this case, the best way to decrease the influence of uncoordinated PEVs charging on a smart grid would be optimal charging.

Here, some studies have been done on PEVs charging coordination [12-13]. If there is high PEV penetration, charging their batteries should be postponed to off-peak hours, so as to overcome the limits of the available generation capacity [13].

There are also other studies that have investigated the impact of PEVs on a grid. In [14], an algorithm was proposed to solve the load flow calculations to examine the impact of Electric Vehicles (EVs) on the distribution system. The impact of high penetration PEVs, on a grid, was improved in Ref [15]. However, the energy prices were not dynamic, and there was no smart strategy. In [16], EV integration into the system and its impact on the electricity market was studied, but the transformer rating and variable charge of PEVs were not considered.

In general, the choice of an optimisation algorithm depends on a variety of factors, such as, the required solution quality, the computing time and the selection of the objective functions, or the problem's constraints. Several conventional optimization methods were used in different studies

to solve the PEV charging coordination problem including Linear Programming (LP), and Dynamic Programming (DP) [17-18]. However, if the problem becomes large, Linear Programming algorithm, cannot address the problem in a reasonable amount of time given the volume of computation.

Additionally, when traditional optimization methods are employed to deal with complicated optimization problems, computational complexities become an issue.

In recent decades, intelligent algorithms such as Genetic Algorithms (GAs) and Particle Swarm Optimization (PSO) have been applied to address complex, real-world power system optimization problems, which involves a large number of possible solutions [19-20].

Many of these methods are based on a group of solutions categorized as population-based methods. Due to its higher efficiency and easier implementation, PSO is adopted for most applications.

In this thesis, due to the discrete nature of the PEV charging coordination problem, the Discrete Particle Swarm Optimisation (DPSO) was implemented. To improve it further, the Coordinated Aggregated Particle Swarm Optimization (CAPSO) was applied to reduce the computation time burden, and improve efficiency.

In this case, PEV penetration and the resulting impact on the electricity market, utilizing a time-of-use scheme, are presented in Ref [21]. The used price was not dynamic and did not follow the real time price schedule. The load demand in relation to the EV battery charging, is modelled in Ref [22], however, the SOC_{Req}, battery modelling, charger size and variable charging, are not considered. Refs [23]-[25] evaluates how the integration of PHEVs/PEVs, impact a grid, using different charging scenarios. Ref [26] investigates the impact of EV, on the power system. Moreover, a series of electric vehicle loads are used to investigate the energy usage in [27].

In order to increase customer satisfaction, different objective functions can be formulated. It can be observed that the customer benefits are increased when considering the demand side management [28], [29]. Refs [30] and [31] use a specific formula to maximise the State of Charge (SOC), for all PEVs. However, neither customer interest, nor the power grid, is referred to. Ref [32] presents a multiagent-based solution for high EV penetration in power systems. In [33], however, the variable charge of the battery, battery modelling and the requested SOC, are not studied. In [34] the objective is benefit maximisation for all customers.

The main purpose of this thesis is to investigate the optimal charging coordination of PEVs within the Smart Grid (SG). The ultimate goal is to maximise customer satisfaction while reducing total power loss and voltage fluctuation, on on-line bases considering the variable charging profile. The proposed approaches are as follows:

Step 1- Employs two online heuristic and dynamic algorithms based on fuzzy genetic algorithm (FGA) and Fuzzy Discrete PSO (FDPSO) to coordinate charging of PEVs. The costs for the generated energy and the grid losses are minimised whilst the power transferred to the PEVs is maximised, subject to the distribution transformer loading, voltage boundaries and SOCs for each battery, at the start time (plug-in time) and the requested final SOC.

Step 2- Implements an online coordinated charging genetic algorithm (OL-CC-GA) using the PEV fixed charging in the SG, which can also perform delayed (e.g., partial-overnight or full-overnight) vehicle charging, by reducing the distribution transformer loading, with the uncoordinated and coordinated PEV charging activities.

Step 3- Designs, codes, and implements a DPSO for PEV charging coordination, taking residential distribution transformer life into consideration.

Step 4- Uses Coordinated Aggregated Particle Swarm Optimisation (CAPSO) to obtain the optimal variable scheduling of the charge rate for PEVs to satisfy the PEV owners' preferences.

1.2. Objectives

This research aims to implement a new OLCC-CAPSO algorithm to coordinate large PEV populations, taking into consideration variable vehicle charging rates to minimise the cost of generating electricity, whilst maximising customer preference. There are three different steps to achieve the objectives of this thesis:

Step 1. Proposing an on-line, fast and reliable coordinated charging of particle swarm optimisation algorithm to reach a near optimal result for PEV scheduling within residential networks.

Step 2. Performing variable charge rates and time-varying energy prices for PEVs to satisfy both consumers (PEV owners) preferences and the regulation of voltage profiles at all buses. It is used based on the designated upper and lower limits of node voltages, including current residential transformer limits.

Step 3. Developing and undertaking PSO, DPSO, FGA and advanced online PSO (CAPSO) based maximisation of customer preferences, in smart grids populated with PEVs, whilst minimising the cost of generating energy, on a number of IEEE test networks.

1.3. Contributions

This research proposes a new OLCC-CAPSO algorithm to manage multiple PEV charging activities, within smart grids, taking into consideration the variable charging capabilities of PEVs. That may impact the grid voltage profile, power losses and the distributed transformers overloading levels, whilst, at the same time, reducing system stresses and increasing customer

satisfaction. The proposed algorithm starts PEV charging as soon as the vehicles are plugged-in, based on an on-line PSO (e.g., every 5 minutes) to maximise total system consumer satisfaction functions and enhance the voltage profile, whilst considering the variable charging capability and opportunity for the PEV owners. The 449-node test system will be simulated, to show the improvement gained by using OLCC-CAPSO. The outcomes of the simulations, such as the system power consumption, voltage profiles for the weakest node in the system at each interval, total system losses and customer satisfaction functions are presented. These findings will be compared and analysed for both uncoordinated and coordinated charging schemes, with 16, 32, 47 and 63 percentage of PEV penetration. The main contributions to this research are:

- On-line coordination of PEVs in the residential system with a random plug-in of vehicles.

- Consideration of variable charge rates for PEVs to satisfy consumer (PEV owners) preferences.

- PSO, GA and advanced PSO (CAPSO) based maximisation of customer preference in smart grids populated with PEVs, whilst minimising the cost of generating the energy required.

- Regulation of voltage profiles at all buses based on designated upper and lower limits.

- Consideration of current residential transformer current limits in the PEV charging coordination problem.

- Consideration of the thermal impacts of using PEVs in a smart grid, distribution transformer loss of life and its acceleration aging.

- Design and coding of OL-CC-GA for online and delayed (full-overnight and partial overnight) PEV charging for a 19-node test feeder.

- Design and coding of CAPSO, using a variable battery charge rate, applying the chargers' efficiency factor, modeling the PEV's batteries and satisfaction of customers. The CAPSO is used according to the requested plug-out time intervals, to the requested final SOC, to their willingness to be charged and pay more for the energy, and driving patterns.

1.4. Thesis Organization

The research carried out is presented in the following chapters:

Chapter 2: On-Line, Full over-night and Partial over-night PEV charging Coordination

This chapter shows an online coordinated charging strategy for PEV using genetic algorithm. This strategy considers partial-overnight and full-overnight charging to reduce distribution system overloading. The proposed coordinated charging strategy has been tested on a 19 node test feeders with a number of PEV units.

Chapter 3: Hybrid Fuzzy Genetic and Particle Swarm Optimization for PEVs charging coordination in the smart grid

This chapter proposes two heuristic based optimization techniques for optimising online charging of PEV units. The proposed techniques maximise the transferred energy while minimising the associated cost and total losses in the system. The techniques are tested on 449-node test system. The results are compared with other methods presented in literature.

Chapter 4: PEVs Battery Fixed and Variable Charging Scheduling in the Smart Grid using Coordinated Aggregated Particle Swarm Optimization, considering Customer Satisfaction

Chapter 4 develops a dynamic online optimization algorithm to achieve an optimal variable charging of PEV units for a given time-slot. The algorithm is based on aggregated Particle Swarm Optimization which achieve the highest customer satisfaction considering customer preferences (e.g. disconnection time, desired state of charge).

Chapter 5: Summary and Conclusions

Chapter 5 concludes the research by highlighting major findings from this research. Major contributions and plenty of directions for future research in this subject are also covered in this chapter.

CHAPTER TWO

ON-LINE, FULL OVER-NIGHT AND PARTIAL OVER-NIGHT

PEV CHARGING COORDINATION

Uncoordinated PEV charging has a significant impact on the power system. When charging is uncoordinated, huge amounts of power will be consumed if a large number of PEVs are connected to the grid at the same time. This, in turn, may cause power losses and overloading, especially during peak hours. PEV charging coordination and transformer capacity should therefore be upgraded [11, 35].

The scheduling of PEV charging can be divided into different groups. The first is the offline pattern for PEV charging coordination, if there is some data available about the future charging demand of PEVs. For online charging, there is no data about future charging demand. However, the advantage of an online mechanism for PEV charging coordination is that it can be made ready for unpredictable charging demand.

2.1. Different Patterns of Charge for PEVs

Charging large PEV fleets will require additional electric power that may lead to undesirable peaks in power consumption, transformer overloading and interruptions. A potential solution is to use appropriate PEV charging coordination strategies [35-38], [39].

The impact which PEVs has on power system losses is investigated in Ref [11], with the use of load modelling. The impact of uncoordinated PEVs charging, on power consumption, is investigated in [39]. In [40], probability density functions are used to identify the PEV charging load. In [41], the queuing theory has been applied to model the charging of PEVs, where Ref [42]

24

considered the uncertainties of charging the PEVs and used the Monte Carlo method to model the charging. Ref [43], introduced a smart charging pattern, in order to minimise the total charging cost of PEVs, the total energy consumed and the losses. Similar to Ref [42], an approach based on the Monte Carlo simulation, was used to evaluate a stochastic modelling of PEVs and their impact on the Dutch distribution system. There are various other studies that have introduced smart methods to charge PEVs, including Refs [44-47]. Ref [48] used deterministic and stochastic studies, to compare the impacts of added loads, due to PEVs within the distribution networks. Another formulation-based stochastic modelling was studied in Ref [49]. In Ref [50], the demand charging level has been predicted for future years, taking into account, the different levels of penetration and the types of PEVs. In Ref [51], a cost minimising strategy is proposed, but does not consider the issue of fairness in the charging of all PEVs. A multi-agent system is proposed in Ref [52], to undertake the PEV charging coordination, using a distributed control algorithm. Ref [53], also implemented a fuzzy method, to solve the multi-objective problem and Ref [54], used the population-based metaheuristic approach to solve the optimisation problems. Another study, Ref [55], also demonstrates that optimising the charging schedule can decrease the number of grid voltage drops and power losses as well as optimising the load profiles.

There are some offline and online charging methods for the charging of PEVs that are based on the current information relating to the future of these vehicles, including the plug-in times and the battery *SOCs*, utilized to decide charging plans. For instance, in Ref [56], it is assumed that all PEVs must communicate their charging timetables to the charging station one day ahead. This coordination approach is not always practical, as it depends on the accuracy and the availability of the predicted PEV information. Furthermore, in many cases, the charging profile will reveal a time that the PEV can connect to the home/car-park outlet.

Ref [37] implements real-time PEV coordinated charging, within the residential distribution systems to reduce the costs of power generation and power losses. Ref [38] presents real-time PEV charging/discharging coordination, without considering customer preferences and variable charge rates. Ref [57] presents real-time charging coordination of PEVs, that is based on the hybrid fuzzy discrete Particle Swarm Optimisation (PSO). In Ref [59] a real-time scheduling method of PEV charging loads is proposed as a way to increase the voltage security margin within an LV distribution system.

There are also some studies conducted into the establishment of a fixed rate for PEV charging. Ref [59], implements an algorithm that considers owners bidding to charge their vehicles. However, all PEVs have a fixed charge rate, which is not usually the case for practical applications, as vehicles have different battery and charger types as well as ratings. Ref [60] presents the online coordination of PEV charging and the discharging methods based on the assumption that PEVs will not arrive when the charging schedule is closed. Ref [32] analyses the performance of optimal PEV charging coordination including customer satisfaction. However, it does not consider the variable charge rates. Refs [61-62] focus on maximising the aggregator revenue without carefully addressing the customers' preferences and thus may not necessarily lead to a maximum benefit for customers. Alonso et al. [63] used GA during on-peak hours to fill the valleys. In addition, Nguyen and Le [64] present an optimisation problem that aims to minimize the total cost of energy of each PEV user. Another method to decrease the impact of uncontrolled PEV charging is presented in Ref [68]. However, Ref [58-59, 63-64] does not include variable charging rates and ignore battery and charger efficiencies. Ref [65] assumes that electric vehicle drivers are insensitive to charging costs and discharging benefits. In addition, Ref [66] presents the integration of wind power and PEV charging.

In fact, the consideration of fixed charge rates for all PEVs is not usually the case for practical applications as vehicles have different battery and charger types as well as ratings. In addition, when the charging coordination takes customer's satisfaction into consideration, some vehicles can request plug-out times and an associated state of charge (SOC_{Req}). Meeting these requirements is not a big problem when all of the vehicles plug out at their requested departure times. However, when unexpected PEV departures occur, conventional schemes such as those proposed in Ref. [37-38, 59-60], may not be able to provide acceptable levels of fairness amongst users. Moreover, there will be cases in which some vehicles may not get the full charge requested by the time of their departure. This problem can be resolved by using variable charging rates as a strategy to adapt the power drawn by the charger from the grid to the load, in order to fully exploit grid capability, and provide a high degree of user satisfaction.

This chapter presents a heuristic-based Online Coordinated Charging Genetic Algorithm (OL-CC-GA). The algorithm used for charging PEV batteries in the SG, which minimises the cost related to the energy generated and minimises the grid losses. It is also increasing the number of charged PEVs, regulating the node voltages and reducing the load of the distribution transformer. OL-CC-GA also takes into consideration any changes to the distribution transformer loading for online and delayed (e.g., full-overnight and partial-overnight) PEV charging. Simulations are performed for a 19-node test feeder that is populated with PEVS using OL-CC-GA. This is then compared with uncoordinated and delayed charging strategies.

2.2. PEV State of Charge (SOC) and battery capacity

The percentage of the available capacity of the vehicle battery is described as SOC in Ref [64] where it can be forecast in regard to the number and length of the PEV trips. In Ref [67-68] the range of battery SOC is identified as ranging between 20% and 90%.

In different studies, the PEVs' battery capacities have been considered in the range of 8kWh to 16kWh. In details, the PEV battery capacities are 8kWh [106], 8.2 kWh [105], 11kWh [11] and 16kWh in [71].

2.3. Vehicle Arrival Time

The usual PEV charging time is a function of the energy cost in ¢/kWh [72], and it is from 21:00h to 07:00h, as owners are expected to park their vehicles at home during those hours. In Ref [73], the owners prefer to charge their vehicles during the night and their charging time will start from 16:00h to 04:00h, while the charging peaks will be at 21:00h.

In Ref [74], two different start times are considered for the PEV charging. The starting time for PEVs is also formulated using a normal probability distribution function (PDF) with a mean starting time of 18:00h and with a standard deviation of one hour.

In this study, it is assumed that the vehicle arrival time is from 16:00h to 23:00h.

2.4. Charging Profile

PEVs can be connected/disconnected at any time according to the customer's needs, and customers can input their preferred plug-out times and requested final SOC at the time of plug-in. PEV owners are also prepared to pay a higher energy price, than the short term market energy price (MEP, Fig.2.1) for their requested charging arrangements. Each hour is divided into 12 time slots of *Δt=5* minutes.

In this study, different PEVs' penetration levels are used, to show the ratio between the number of PEVs and the low-voltage residential nodes.
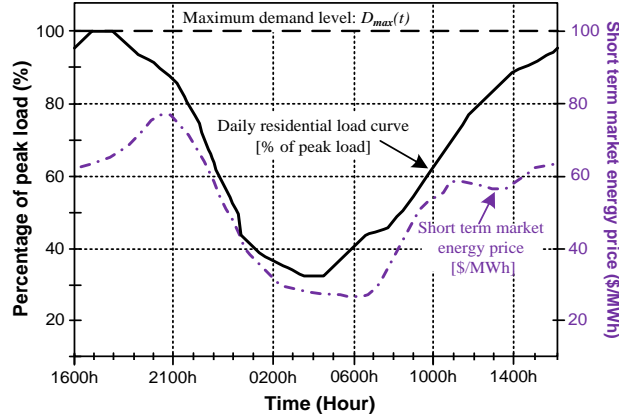
Fig. 2.1. System characteristics: daily residential load curve (DLC) and short term market energy price (MEP) [37]

2.5. Heuristic Algorithm to Solve Optimisation Problem

2.5.1. Initial Population and Fitness Function

In this chapter, if the PEV is being charged, then its status will be '1', if not it is '0', which shows that the charging has either not been started, or has already finished. Fig. 2.2(c) shows the proposed structure of the GA chromosome.

2.5.2. GA Fitness Function

The inverse algebraic product (Eq. 2.1) of the proposed penalty functions for voltage (Eqs. 2.2-2.3) and demand (Eq. 2.4) is used as the fitness function to combine the PEV charging coordination objective function (Eq. 2.5) and constraints (Eqs. 2.6-2.7).

$$F_{fitness}(t) = F_F(t)/(F_V(t) \times F_D(t)) \tag{2.1}$$

$$F_V(t) = \prod_{k=1}^{n} F_{V,k}(t) \tag{2.2}$$

$$F_{V,k}(t) = \begin{cases} e^{\alpha_{V1}(1-V_k(t))}, & V_k(t) \leq V_{\min} \\ 1, & V_{\min} \leq V_k(t) \leq V_{\max} \\ e^{\alpha_{V2}(V_{\max}-1)}, & V_k(t) \geq V_{\min} \end{cases} \qquad (2.3)$$

$$F_D(t) = \begin{cases} 1, & D_{total}(t) \leq 1 \\ e^{\alpha_D(D_{total}(t)-1)}, & D_{total}(t) \geq 1 \end{cases} \qquad (2.4)$$

where $F_V(t)$, $F_D(t)$ and $F_F(t)$ are the bus voltage penalty function, the demand (distribution transformer loading) penalty function and the objective function at time t, respectively; α_{V1}, α_{V2} and α_D are the coefficients used to adjust the slopes of the penalty functions.

The selected values for parameters α_{V1}, α_{V2} and α_D are 0.85, 0.8 and 0.75.

The voltage and demand penalty functions are demonstrated in Figs. 2.2(a) and 2.2(b), respectively.

(a)   (b)

(c)
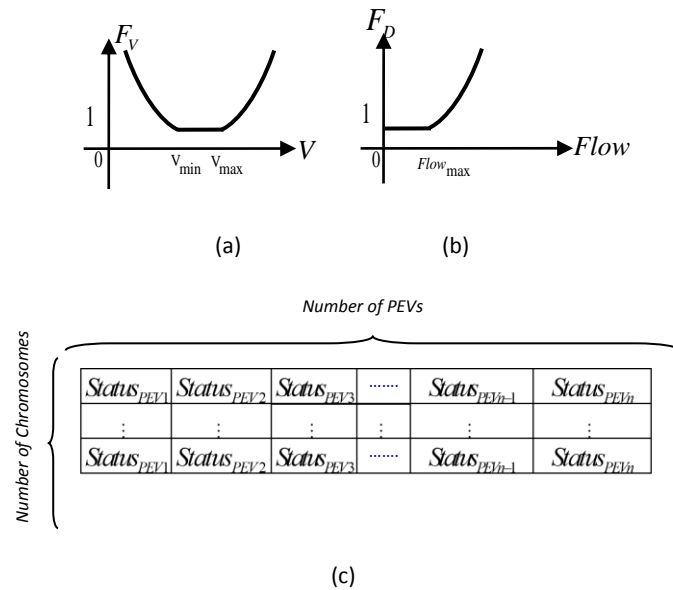
Fig. 2.2. Penalty functions to compute fitness (a) F_V , (b) F_D , and the proposed structure of the GA chromosome (c) [75]

30

2.6. Binary Genetic Algorithm Operators

Genetic operators usually consist of three different parts, including crossover, mutation, and reproduction. In this chapter, these three parts will apply to the chromosomes in each stage of optimisation to produce a new enhanced population [76].

The mechanism used for reproduction in this study is a roulette wheel. In addition, there are some characters at the crossover points either left or right, and they will be swapped during the optimisation. A string position will be improved by changing 0 to 1 using a minor probability in the mutation section.

2.7. Proposed GA at Each Time Slot (Δt)

The proposed Online Coordinated Charging Genetic Algorithm (OL-CC-GA) for PEVs in SG consists of eight steps:

Step 1: Enter all the parameters for the test system and the optimisation data. Read smart meters to check PEV entry time and location for newly connected PEVs.

Step 2: Assume N_{Ch_max} and N_{it_max}. Establish required initial counters and set their values (e.g., $N_{Ch}= N_{it}=1$). Initialise the position and velocity vectors using a random generator.

Step 3 (Fitness Evaluation Process):

Step 3A: For each set of chromosomes, it is required to run a power flow and the objective function (Eq.2.5) should then be computed.

Step 3B: Compute the proposed penalty functions (Eqs. 3.9-3.11).

Step 3C: If $N_{ch} \leq {}_{Nch\text{-}max}$, go to step 3A.

Step 4 (Reproduction Process):

Step 4A: Define total fitness as the product of all fitness values for all chromosomes.

Step 4B: Run a tournament for the selection process. Select a new combination of chromosomes.

Step 5 (Crossover Process):

Step 5A: Select a random number (R_1) for mating two parent chromosomes.

Step 5B: If R_1 is less than the values of the crossover, then combine the two parents, generate two offspring and go to Step 5D.

Step 5C: Otherwise, transfer the chromosome with no crossover.

Step 5D: Repeat Steps 5A to 5D for all chromosomes.

Step 6 (Mutation Process):

Step 6A: Select a random number (R_2) for the mutation of one chromosome.

Step 6B: If R_2 is less than the values of mutation, then apply the mutation process and go to Step 6D.

Step 6C: Otherwise, transfer the chromosome with no mutation.

Step 6D: Repeat Steps 6A to 6C for all chromosomes.

Step 7 (Updating Population):

Replace the old population with the improved population generated by Steps 2 to 6. Check all chromosomes. If there is any chromosome with $F_L=1$, $F_G=1$, $F_V=1$, $F_D=1$ and $F_F>F_{max}$, set $F_{max} = F_F$ and save it. Set $N_{it}=N_{it}+1$.

Step 8 (Stopping Decisive Factor):

If the maximum number of iterations is achieved, then start PEV charging and go to the next time slot.

2.8. Fitness Function

Online coordination of PEV charging is a real-time optimisation problem that requires formulation

of a comprehensive objective function and a high-speed optimisation method to quickly capture the best solutions. In this chapter, the nonlinear objective function of Eq. 2.5 is defined for the PEV charging coordination problem to maximise the number of vehicles that are being charged ($N_{PEV\text{-}ON}$) at each time slot ($\Delta t = 5\,min$), whilst also minimising the costs associated with energy generation ($F_{cost\text{-}gen}(t)$) and grid losses ($F_{cost\text{-}loss}(t)$) [37]:

$$max\ F(t) = \frac{1 + N_{PEV-ON}(t)}{F_{cost-gen}(t) + F_{cost-loss}(t)} =$$

$$\frac{1 + N_{PEV-ON}(t)}{\sum_t K_E\, P_{loss}(t) + \sum_t K_{t,G}\, D_{total}(t)}, t = \Delta t, 2\Delta t,..24\,hours \qquad (2.5)$$

$$where,\ P_{loss}(t) = \sum_{k=0}^{n-1} R_{k,k+1} \left(\left\| V_{k+1}(t) - V_k(t) \right\| y_{k,k+1} \right)^2.$$

Eq. 2.5 is subject to the following voltage and demand (transformer loading) constraints:

$$V_{min} \leq V_k(t) \leq V_{max},\ \ for\ k = 1,...,n \qquad (2.6)$$

$$D_{total}(t) = \sum_{k=1}^{n} P_k(t) = \sum_{k=1}^{n} (P_{Load_K}(t) + P_{PEV_K} \leq D_{max}(t) \qquad (2.7)$$
$$t = \Delta t, 2\Delta t,....$$

$$where\ D_{max}(t) = Max\{DL(\Delta t), DL(2\Delta t),...,DL(m\Delta t)\}$$
$$m = 1,...288$$

In Eqs.2.5, $\Delta t = 5\,min$ is the time interval; $K_E{=}50\$/MWh$ and $K_{t,G}$ are the costs per MWh of loss [37] and generation (Fig. 2.1) respectively; k and n are the node number and the total number of nodes; $R_{k,k+1}$ and $y_{k,k+1}$ are the resistance and reactance of the line segment between nodes k and $k{+}1$, respectively; V_{min} and V_{max} are the lower and upper voltage limits, respectively; $D_{max}(t)$ is selected to be 0.84MW corresponding to the maximum load for the selected DLC. $P_{Loadk,}$ is the base-load power, DL is the daily load at m^{th} time slot, and P_{PEVk} is the consumed power for the PEV at node k. The backward-forward sweep method is used to calculate load flows and bus voltages [77].

- The proposed OL-CC-GA is modified to allow for both online and delayed PEV charging coordination strategies:

- Online Coordination — vehicles are charged as soon as possible as they are being plugged-in. This will result in high customer satisfaction levels, at higher energy prices.

- Delayed Full-Overnight Coordination — vehicle charging is delayed and performed during early morning hours to reduce the charging costs. This may result in less customer satisfaction as some PEVs may not be fully charged overnight for the next trip.

- Delayed Partial-Overnight Coordination — Some PEVs (e.g. high priority vehicles) will get charged at the time of being plugged-in, while the rest will be postponed for overnight charging.

- To allow for delayed PEV charging, the value of $D_{max}(t)$ in Eq. 2.8 is modified. For delayed full-overnight charging $D_{max}(t)$ is a constant and is computed by trial and error; $D_{max}(t) = D_{ovrnight}$ =31.1kW. For delayed partial-overnight charging, $D_{max}(t)$ is computed using the following linear equations [75]:

$$\begin{cases} D_{\max}(t) = 43.73(0.85 - 0.025 \times (t - 12:00)); & 06:00^{PM} \leq t < 11:59^{PM} \\ D_{\max}(t) = 43.73(0.65 - 0.025 \times (t - 8:00)); & 00:00^{AM} \leq t \leq 08:00^{AM} \end{cases}$$

(2.8)

where the peak load for this test system is 43.73 kW.

2.9. Simulation Results and Discussions

The 19-bus 415V distribution test system of Fig. 2.3 populated with PEVs is used to evaluate the accuracy of the implemented algorithms (Figs. 2.4-2.5 and Table 2.1).
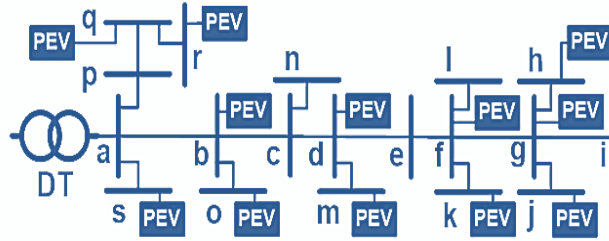
Fig. 2.3. The 19-node 415V residential feeders with PEVs [75].

Case A. Uncoordinated PEV Charging

The uncoordinated charging of PEVs causes increases in power usage, generated power, voltage violations and in total system losses. The results are shown in Figs. 2.4 (a-c) and Table 2.1.

As expected, the network is facing overloading, voltage regulation and efficiency problems. As an example, for 100% PEV penetration, maximum power consumption and maximum system losses were recorded and the cost increased by about 89% (Fig. 2.4(a)), 247% (Fig. 2.4(c)) and 110% (Fig. 2.4(b)), respectively; compared to the nominal operation with no PEVs.

Case B. Coordinated Online (OL-CC-GA) PEV Charging

For further investigations into the performance and accuracy of uncoordinated charging, the online PEV charging coordination strategy, based on the GA is proposed. Simulation results are shown in Fig. 2.4 and Table 2.1 (rows 6-7). Compared to Case A, GA is offering a further reduction in transformer overloading (Fig. 2.4(a)), when the maximum generation cost level reduced from 5.68$ (Fig.2.4 (b)) to 2.68$ (Fig. 2.4(b)). In addition, in this case, the maximum system losses and the total cost reduced from 3.27KW to 1.12KW, and 46.31$/day to 42.44$/day, respectively.

Case C. Coordinated Delayed Partial-Overnight PEV Charging

The proposed OL-CC-GA is modified to allow for delayed partial-overnight PEV charging using Eq. 2.8. Simulation results are shown in Fig.2.5 and Table 2.1 (rows 8-9). The performance of partial-overnight PEV charging is different from the uncoordinated and online strategies. Total system losses are significantly reduced when compared to case B. However, there is a 10% voltage variation, and the total power consumption in the system is less than the allowable demand level.

(a)

(b)

36

(c)
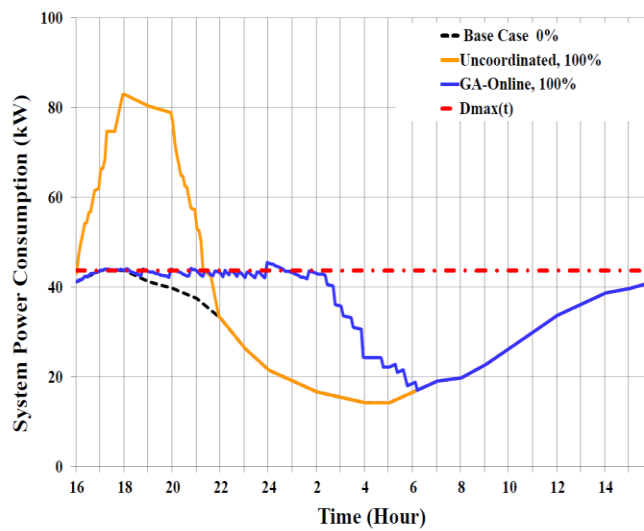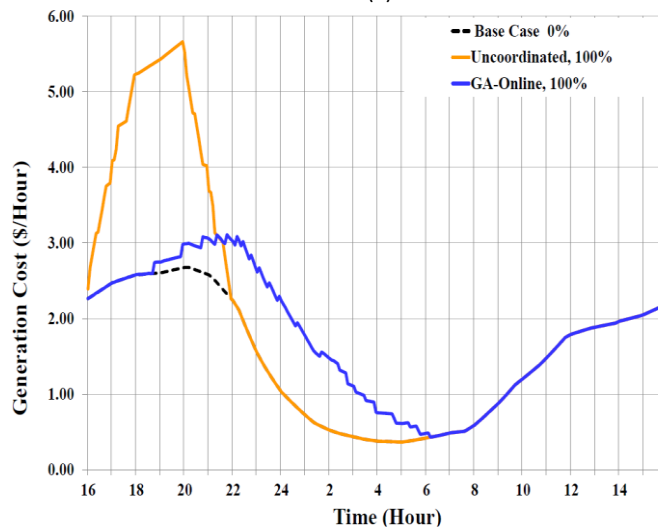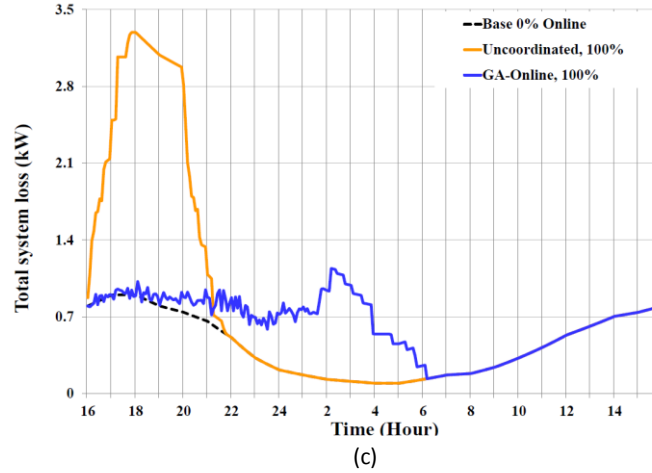
Fig. 2.4. Simulation results for Cases A-B with 0% and 100% PEV penetrations: (a) system power consumption, (b) generation cost, (c) total system losses [75].

Table. 2.1. Impact of uncoordinated, online coordinated (OL-CC-GA) and delayed coordinated PEV charging, on the test feeder of Fig. 2.3.

PEV [%]	ΔV* [%]	I MAX** [%]	Generation cost [$/day]	Total cost [$/day]	Increase in Total cost [%]
Nominal Case: With no PEV (0% PEV penetration)					
0	7.63	0	35.13	36.6	0
Case A: Uncoordinated PEV Charging; Fig. 2.4					
100	16.10	89	46.31	49.75	26.53
Case B: Online PEV Charging (OL-CC-GA); Fig. 2.4					
100	9.89	0	42.44	44.93	15.95
Case C: Partial-Overnight PEV Charging (Modified OL-CC-GA); Fig.2.5					
100	9.78	0	41.06	43.37	12.18
Case D: Full-Overnight PEV Charging (Modified OL-CC-GA); Fig. 2.5					
100	9.72	0	40.20	42.18	9.83

*) Average voltage deviation over 24 hours (Eq. 2.2).
**) Increase in transformer current compared with the nominal case.

Case D. Coordinated Full-Overnight PEV Charging

In this particular scenario, it is demonstrated that all PEVs will be queued, whilst the aggregators coordinate the overnight charging, resulting in all PEVs being fully charged by 08:00. To modify the OL-CC-GA for full-overnight PEV charging, $D_{max}(t)$ is a constant and its value is computed by trial and error to be $Dovrnight = 31.1$kW.

The performance of full-overnight PEV charging is better than Cases A-C as the total system losses are significantly reduced and voltage fluctuations are still within the 10% limit.

37
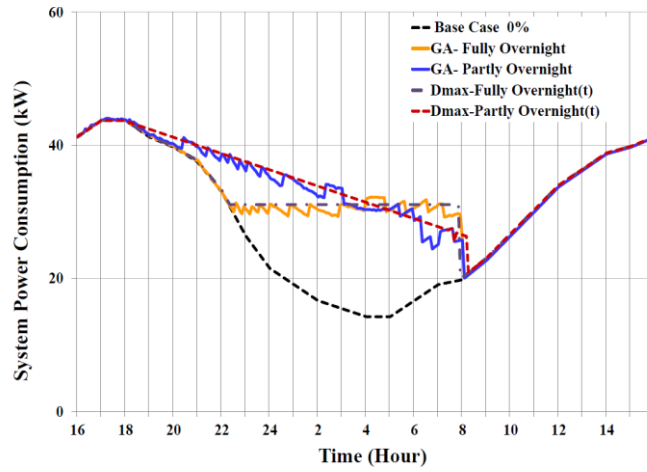
(a)
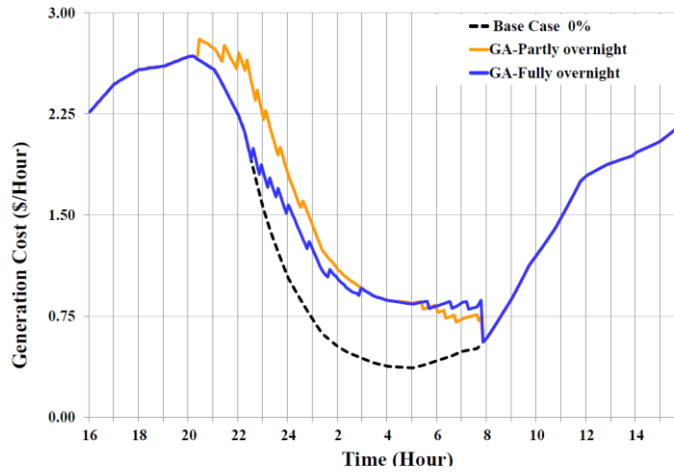
(b)
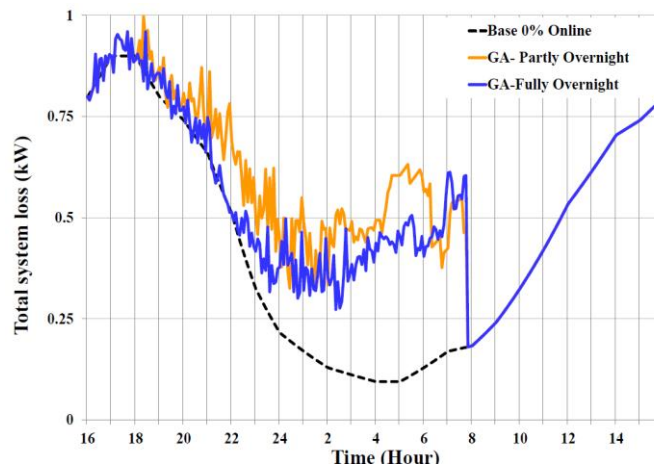
(c)

Fig. 2.5. Simulation results for Cases C-D with 0% and 100% PEV penetration: (a) system power consumption, (b) generation cost, (c) total system losses [75].

2.10. Summary

- An Online Coordinated Charging Genetic Algorithm (OL-CC-GA) for PEVs in the SG was created so that it can also perform delayed (e.g., partial-overnight or full-overnight) vehicle charging by reducing the distribution transformer loading. Detailed simulation results for a 19-node test feeder are presented and compared with uncoordinated, online, delayed partial-overnight and delayed full-overnight PEV charging. The main conclusions are:

- The proposed OL-CC-GA schedules the charging activities of randomly arriving PEVs at each time slot, based on smart meter information using online cost minimisation. The modified OL-CC-GA takes advantage of this expert knowledge to vary the distribution transformer loading level ($D_{max}(t)$ in Eq. 2.7). It performs delayed PEV charging by postponing some vehicle charging such that the peak power consumption is shifted to the early morning hours to achieve further reductions in total costs.

- In OL-CC-GA, the total system cost achieves maximum value in Cases B, C and D; however, all PEVs will be charged before 06:00. In addition, Case B has the maximum losses amongst the all of the coordinated cases, whilst the generation cost of Case D has the minimum losses, compared to the other cases.

- In delayed partial-overnight PEV charging coordination, the generation cost is higher than Case D and lower than Case B.

CHAPTER THREE

HYBRID FUZZY GENETIC AND PARTICLE SWARM OPTIMISATION FOR PEVS

CHARGING COORDINATION IN A SMART GRID

The interest of electric utilities and the public in a smart grid has increased in line with increasing concerns about the environment. If PEV charging is coordinated smartly, then this type of vehicle will be more beneficial and more cost-effective for the customer and for public utilities [78]. PEV charging in general can be categorised by centralised [11, 37, 44, 79-83] and/or decentralised coordination schemes [32, 84-87].

Two dynamic centralised heuristic approaches that are based on hybrid FGA and FDPSO have been proposed to optimise the online charging of PEVs in a smart grid. The proposed algorithm maximises the transferred energy to the PEVs whilst also minimising the costs associated with the energy used and the total losses in the system. This is while satisfying required voltage regulation for all nodes and reduce the load on the distribution transformer.

 The simulation results of the test system (449-node) are illustrated and compared with MSS [16], GA, DPSO, FGA and FDPSO methods.

3.1. Problem Formulation

PEV charging coordination is a complex real-time and time-dependent problem. To achieve a speedy optimized solution, this chapter proposes a heuristic-based optimization technique with a comprehensive objective function.

In this thesis, the charging status for the PEVs has been selected as the optimisation variable where it is assumed that charging rates are different and variable for each PEV. In details, a C-rate is a measurement of the rate, at which a battery is charged or discharged, relative to its maximum

capacity. A 1C rating means that the battery will fully charge/discharge in 1 hour. In this research, variable charging rates have been used, whereas for the fixed charging, it is the ratio of the power rating of the charger/the ampere-hour of the battery which is kW/kWh= 1/hour.

In variable charging cases, it is assumed that the C is a variable between 0 to 2.

It is also considered that within the charging process, that the charge rate for each PEV will stay constant. E.q. 3.1 presents a nonlinear objective function for the charging coordination of PEVs to maximise the total power delivered to PEVs, at each time interval ($\Delta t=5$ minutes), whilst the cost of the generation ($F_{cost\text{-}gen}(t)$) and total system losses ($F_{cost\text{-}loss}(t)$) are minimised. The objective function in Eq. 3.1 is subject to the power required for each time slot (Eq. 2.7), SOC constraints (Eq. 3.2) and voltage deviations to secure the quality of the supplied power for the base load and the PEV loads.

$$Max\,F(t) = \frac{F_{DCP}(t)}{F_{\cos t-loss}(t)+F_{\cos t-gen}(t)} = \frac{\sum_{i=1}^{N_{PEV}}\big(\text{Delivered Charging Power}(i,t)\big)}{\sum_{t}K_{E}P_{loss}(t)+\sum_{t}K_{t,G}D_{total}(t)} \qquad (3.1)$$

for t=Δt, 2Δt,...24 hours where $K_{t,G}$ and K_E are generation (Fig. 2.1) and the costs per *MWh* of losses [83], respectively.

$$SOC(i,t) \le SOC_{\mathrm{Re}q}(i) \le SOC_{\max}\,,\,i=1,...,N_{PEV} \qquad (3.2)$$

In this thesis, *SOC (i,t)* presents the SOC for the ith PEV at t, $SOC_{Req}(i)$ is the required SOC for the ith PEV, $SOC_{\max}$ is the state of charge of each battery and $SOC_{initial}$ at plug-in time is based on the driving scheme for each PEV [88]:

$$F(t)=\begin{cases}\alpha_{i}-(\alpha_{i}-\beta_{i})\times\dfrac{L_{j}}{L_{i}^{\max}} & L_{j}\le L_{i}^{\max} \\ \beta_{i} & otherwise\end{cases}\qquad for\ i=1,2,3\quad,\quad j=1,.....,N_{PEV} \qquad (3.3)$$

Where, *i* indicates the type of PEVs, *j* is the number of PEVs, L_j is the length of trip path for j^{th} PEV and $L_i^{\max}$ is the rated length path for each PEV [88].

The PEV models used in this thesis were a Volkswagen e-golf (Type 1), a Honda Fit (Type 2) and a Ford C-Max (Type 3). The charger ratings were 7.2, 6.6, and 3.3 kW respectively, correspond to battery sizes of 24, 20, and 7.6 kWh [57]. The selected values for parameters α_1, α_2 and α_3 are 0.85, 0.8 and 0.75 miles; for β1, β2 and β3 are 0.15, 0.2 and 0.25miles; and for L_1, L_2 and L_3 are 40, 50 and 60 miles, respectively.

The information required for each PEV, such as charger type, battery capacities, $SOC_{initial}$, SOC_{Req} and the location of each PEV was provided using the smart meters and sent to the aggregator. The scheduling horizon started at 16:00 (arrival time for most of the PEVs) for the next 24 hours, and each day was divided into 288 time intervals ($\Delta t=5$ minutes).

The backward/forward sweep power flow method was used to calculate the voltage and load flows [11]. It was assumed that the amount of generation was sufficient to provide energy for the base load and for charging the PEVs. In a case where an owner would charge the PEV without requiring the schedule, that PEV would be assumed to be part of the daily load base.

3.2. Proposed PEV Charging Method

Two different approaches based on fuzzy rules, namely DPSO and GA, were deployed in this thesis to optimise Eqs.3.1-3.2, 2.6-2.7; this was because most of the practical optimisation problems, such as PEV charging coordination, required a discrete optimisation solution [89].

3.2.1. DPSO Formulation

The DPSO and PSO algorithms are very similar except for the state equations presented in (Eqs.3.4- 3.6). Personal and social coefficients are the bases for the probability function in making decision such as 'yes' or 'no', 'true' or 'false' [90]:

$$P(X_{pt,j}^{it+1}=1) = f(X_{pt,j}^{it}, V_{pt,j}^{it}, pbest_{pt,j}, gbest_j) \tag{3.4}$$

where $X_{pt,j}^{it}$ is the position of the particle pt in the current generation, $pbest_{pt,j}$ is the best point found by particle pt in its past life up to the current generation, $gbest_j$ is the best overall point found by the swarm of particles in their past life and $V_{pt,j}^{it}$ is the agent's choice tendency. The sigmoid function that achieves this threshold is:

$$sig(V_{pt,j}^{it}) = \frac{1}{1+exp(-V_{pt,j}^{it})} \tag{3.5}$$

To formulate the DPSO, Eqs. 3.6(a) and 3.6(b) were used [91]:

$$V_{pt,j}^{it+1} = V_{pt,j}^{it} + rand_1(pbest_{pt,j} - X_{pt,j}^{it}) + rand_2(gbest_j - X_{pt,j}^{it}) \tag{3.6a}$$

$$if \ \rho_{pt,j}^{it+1} < sig(V_{pt,j}^{it}) \ then \ X_{pt,j}^{it+1}=1, else \ X_{pt,j}^{it+1}=0 \tag{3.6b}$$

where $rand_1$ and $rand_2$ were positive random numbers generated from a uniform distribution [89-90] with a predefined upper limit, while $\rho_{pt,j}^{it+1}$ was a random number between 0 and 1.

Eqs. 3.4-3.6 were used in an iterative procedure over each j dimension of each particle to arrive at a near-global solution. The maximum value of $V_{pt,j}^{it}$ was often limited to [-4, +4] to ensure that $sig(V_{pt,j}^{it})$ did not get too close to the interval limits [0, 1].

3.2.2 Structure of Particles and initial population in DPSO

In this thesis, each particle includes the status of all PEVs where the digit '1' indicates that the PEV has been plugged in and '0' indicates that the PEV has not been plugged in or has already finished charging. The structure of the initial population is identified as follows:

$$\text{Number of population} \begin{pmatrix} Status_{PEV\,1} & Status_{PEV\,2} & ..... & Status_{PEV\,n} \\ Status_{PEV\,1} & Status_{PEV\,2} & ..... & Status_{PEV\,n} \\ \vdots & \vdots & \vdots & \vdots \\ Status_{PEV\,1} & Status_{PEV\,2} & ..... & Status_{PEV\,n} \end{pmatrix} \quad \text{Number of PEVs}$$

(3.7)

3.2.3 DPSO Fitness Function

Fuzzy fitness functions were applied to the objective function and the constraints (Eqs. 3.1- 3.2, 2-6-2.7) to achieve a greater cost reduction and enhance the quality of the results. To mix the PEV charging coordination objective function and the constraints, the inverse algebraic product of the penalty functions for overloading the distribution transformer and voltage deviation was used.

$F(t)$ was the objective function, $F_V(t)$ was the penalty function for the voltage deviation at each bus and $F_D(t)$ was the penalty function for the overloading distribution transformer at each time interval. The inverse algebraic product (Eq. 3.8) of the proposed penalty functions for voltage (Eqs. 3.9-3.10) and demand (Eq. 3.11) was used as the fitness function to combine the PEV charging coordination objective function (Eq. 3.1) and constraints (Eqs. 3.2, 2.6-2.7):

$$F_{fitness}(t) = \frac{F(t)}{F_V(t) \times F_D(t)}$$

(3.8)

$$F_V(t) = \prod_{k=1}^{n} F_{V,k}(t)$$

(3.9)

$$F_{V,k}(t) = \begin{cases} e^{\alpha_{V_1}(1-V_k(t))} & V_k(t) \leq V_{min} \\ 1 & V_{min} \leq V_k(t) \leq V_{max} \\ e^{\alpha_{V_2}(V_k(t)-1)} & V_k(t) \geq V_{max} \end{cases}$$

(3.10)

$$F_D(t) = \begin{cases} 1, & D_{total}(t) \leq D_{fuzzy}(t) \\ e^{\alpha_D(D_{total}(t)-D_{fuzzy}(t))}, & D_{total}(t) \geq D_{fuzzy}(t) \end{cases}$$

(3.11)

$D_{fuzzy}(t)$ was the calculated and adjusted the maximum demand level according to the fuzzy rules

and membership function in Figs. 3.1; α_{V1}, α_{V2} and α_D were the factors used to adjust the gradient of the penalty functions.

3.2.4 Adjusting Maximum Level of Loading Using Fuzzy Expert System (FES)

In this thesis, the fuzzy expert system was used to reduce the cost associated with generation cost $F_{cost\text{-}gen}(t)$ (Eq. 3.1) to calculate the allowable demand level for each time slot. This fuzzy system was also used to determine the demand in the penalty function of Eq. 3.11. There are three levels in the proposed FES of Fig. 2.1, (low (L), medium (M) and high (H)) for the membership functions of DLC, MEP, time and the number of PEVs as input variables. In Fig 3.1 (a), the load is presented in per-unit, and the low level (LV) is considered to be from zero to 0.67pu of the maximum load in a day. While the load increases from the minimum to its maximum, the weight of the medium membership function increases from 0 to 1. The high membership function will impact on the decision engine when the load is at least 0.67pu.

Similar to the DLC, three membership functions have been defined for the market energy price which is from (\$2.4)/ (5-min) to (\$6.5)/ (5-min) (Fig 3.1(b)). The average price is also \$4.4 for each 5 minutes.

The third sets of the membership functions are defined to illustrate the impact of remaining time to charge all PEVs (Fig 3.1(c)). According to this figure, from midnight till 8:00AM is defined as "High", as the PEV owners may need their EVs by 8:00AM. This will provide the highest priority to charge all the remaining PEVs using the proposed optimization algorithm.

The fourth membership function sets (Fig 3.1(d)) consider the impact of Npev on the proposed algorithm. When the number of plugged-in EVs are more than 140, all remaining EVs within the time frame regardless of the time and the energy price will have the highest priority to get charged.

A nine-level output membership function, including extreme low (XL), very low (VL), medium low (ML), high low (HL), medium (M), low high (LH), medium high (MH), very high (VH) and extreme high (XH), were used to adjust $D_{fuzzy}(t)$ at each time slot (Figs. 3.1(a-e). Figs. 3.1(f-h) illustrate the fuzzy surface for the variation of $D_{fuzzy}(t)$ according to the changes on DLC- Npev, DLC-time, and Npev-time respectively. The graph of (MEP-DLC) is shown in Fig 3.1(f). According to this figure, the allocated value for the Dfuzzy(t) is changing from 0.1 to 0.5. The Dfuzzy(t) is set to 0.5 where the DLC and the MEP are at their minimum to provide a higher chance to the aggregator to charge the PEVs. It can also be seen that the variation of the Dfuzzy(t) is linear with the variation of the DLC and MEP.

According to the figures (3.1(f-h)), it is shown that the lower demand level is assigned to $D_{fuzzy}(t)$ for the early evening hours when the market energy price and daily load curve are at their maximum. Furthermore, it can be seen that for the early morning hours to increase the chance of fully charging the PEVs, the demand level assigned to $D_{fuzzy}(t)$ would be higher and would take advantage of lower MEP and DLC (Fig. 3.1(f)).

Based on Fig. 3.1(h), it is shown that the aggregator may require charging more PEVs, when the number of PEVs increases during peak hours to prevent the chance of overloading the distribution transformer later on. Depending on the outcomes of the fuzzy method proposed in this thesis, the total charging cost for a day (24 hours) would be reduced.

(a)   (b)
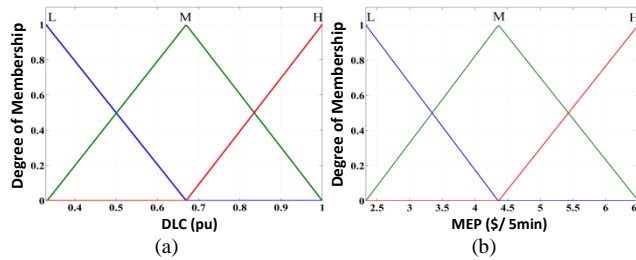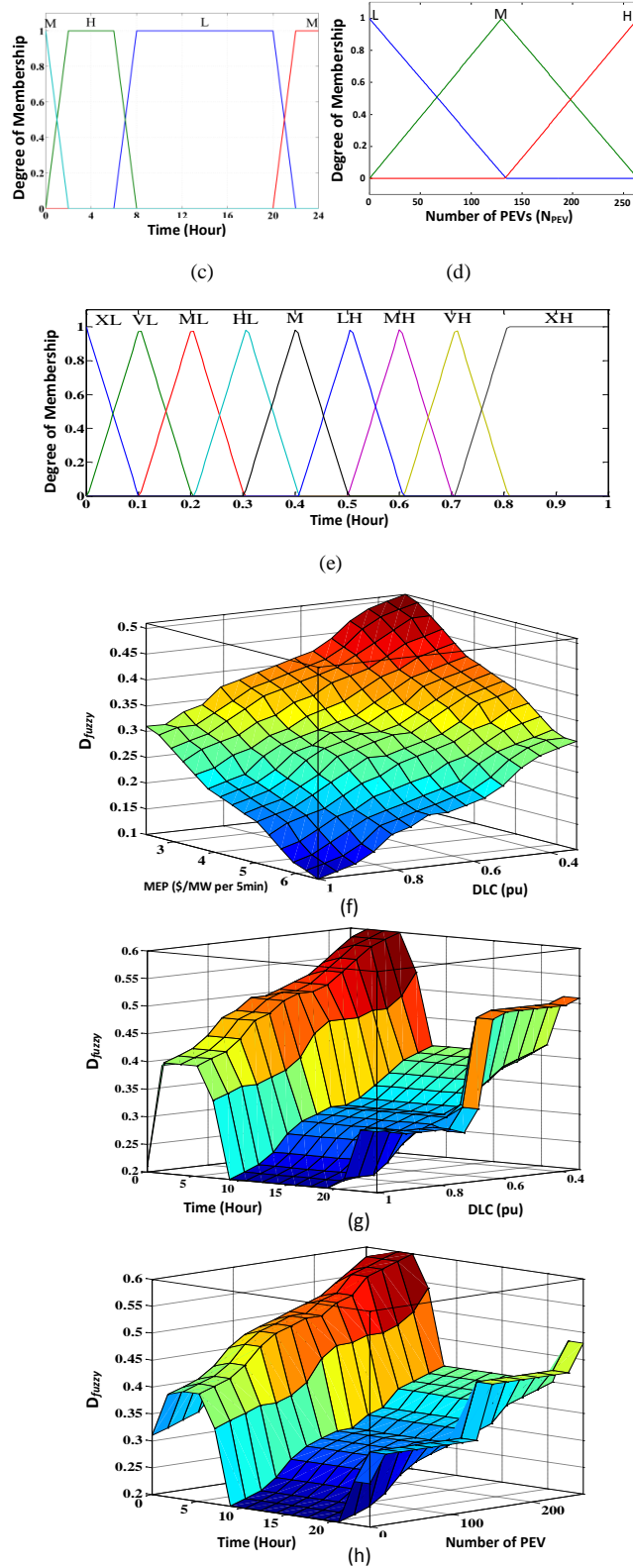
Fig. 3.1. Proposed FES membership functions for: (a)-(e) the three-level inputs DLC, MEP (Fig. 2.1), time and Npev, (e) the nine-level output of D_{fuzzy}, fuzzy surfaces for $D_{fuzzy}(t)$ variations based on: (f) DLC and MEP, (g) DLC and time, (h) Number of PEV and time [57].

3.2.5 Flow Chart of Proposed FDPSO Algorithm

A flowchart of the proposed FDPSO based optimisation using the objective function given in Eqs.3.1-3.2, 2.6-2.7, 3.8-3.11 and Figs. 3.1, is also presented. *Npop* and N_{it} in this flowchart represents the PSO population size and the number of maximum required iterations, respectively.

3.2.6 Proposed Hybrid Fuzzy Genetic Algorithm (FGA)

According to Fig. 3.1, the hybrid FGA is used to show the quality and performance (speed) of the proposed online FDPSO. The two-point crossover and a uniform mutation were used in this thesis to generate the next generation [35]. In addition, a tournament-based selection method was applied to select the paths. The probabilities for crossover and mutation were 0.9 and 0.05 respectively. The flowchart in Fig. 3.2(b) details the proposed FGA for PEV charging coordination according to Eqs. 3.1-3.2, 2.6-2.7 and 3.8-3.11.

(a) FDPSO

Input optimisation parameters (including N_{pop} and N_{it_max}) and power system data (including DLC and price). Set Δt=0.

Read smart meters to check PEV entrances time and location, the current and requested battery state of charge, the battery sizes and charger types.

The initial position ($X_{pt,j}$) and the velocity ($V_{pt,j}$) vectors generated using a random generator. Set $pbest_{pt,j}$ = $X_{pt,j}$. Set $gbest_j$ = $X_{pt,j}$.

Compute the $D_{fuzzy}(t)$ using the proposed fuzzy membership functions in Fig.3.3. Set $N_{particle}$=0. Set N_{it}=0.

Run power flow. Compute objective function (Eq. 4.1). Check constrains (Eqs. 2.6-2.7, 3.1-3.2). Compute fitness function (Eqs. 3.8-3.11).

No — Is Fitness ($X_{pt,j}$) > Fitness ($pbest_{pt,j}$)?
Yes

Set $pbest_{pt,j}$ = $X_{pt,j}$.

No — Is Fitness ($X_{pt,j}$) > Fitness ($gbest_j$)?
Yes

Set $gbest_j$ = $X_{pt,j}$.

Set $N_{particle}$=$N_{particle}$+1.

No — Is $N_{particle}$> N_{pop}?
Yes

Set $N_{particle}$=0.

Update the position of the particle (Eq. 4.6-4.8).

Set $N_{particle}$=$N_{particle}$+1.

No — Is $N_{particle}$> N_{pop}?
Yes

Set N_{it} = N_{it} +1.

No — Is N_{it} > N_{it_max}?
Yes

Start charging the best selected PEVs. Disconnect charged PEVs. Update loads. Set Δt=Δt+5min.

(b) FGA

Input optimisation parameters (including N_{pop} and N_{it_max}) and power system data (including DLC and price). Set Δt=0.

Read smart meters to check PEV entrances time and location, the current and requested battery state of charge, the battery sizes and charger types.

Initial population ($X_{pt,j}$) is generated using a random generator. Set Mutation probability =0.05 and crossover probability=0.95.

Compute the $D_{fuzzy}(t)$ using the proposed fuzzy membership functions in Fig.3.3. Set N_{ch_max} =50. Set N_{it}=100. Set N_{ch}=0.

Run power flow. Compute objective function (Eq. 4.1). Check constrains (Eqs. 2.6-2.7, 3.1-3.2). Compute fitness function (Eqs. 3.8-3.11).

Set N_{ch} = N_{ch} + 1.

No — N_{ch} >N_{ch_max}
Yes

Set N_{ch} =1

Select two chromosomes based on "*tournament*" mechanism. Set N_{ch}= N_{ch} + 1

No — N_{ch} >N_{ch_max}
Yes

Set N_{ch} =1

Select a random number (RND). If RND < P_c then apply the two-point crossover to the chromosome. Set N_{ch}= N_{ch} + 1.

No — N_{ch} >N_{ch_max}
Yes

Set N_{ch} =1

Select a random number (RND). If RND < P_m then apply the single-point mutation to the chromosome. Set N_{ch}= N_{ch} + 1.

No — N_{ch} >N_{ch_max}
Yes

Set N_{ch} =1

Run power flow. Compute objective function (Eq. 3.1). Check constrains (Eqs. 2.6-2.7, 3.1-3.2). Compute fitness function (Eqs. 3.8-3.11).

No — N_{ch} >N_{ch_max}
Yes

If objective function>F_{max} Then Set F_{max} = objective function. Repeat this for all chromosomes.

N_{it}= N_{it} + 1.

No — N_{it} > N_{it_max}
Yes

Start charging the best selected PEVs. Disconnect charged PEVs. Update loads. Set Δt=Δt+5min.

(a) (b)

Fig. 3.2. Flow charts of the proposed algorithms for the online PEV charging coordination, (a) FDPSO, (b) FGA

3.3. The 449-Node Test System Smart Grid

To evaluate the quality and performance of the proposed methods, including FDPSO and FGA, the test system shown in Fig. 3.3 was used. This test system was the modified IEEE 31 bus 23 kV with 22 LV residential feeders. Each feeder included a 19 node test system which represented the customer households. All of the detail, such as line data and load information for all residential feeders can be found in Ref. [37].

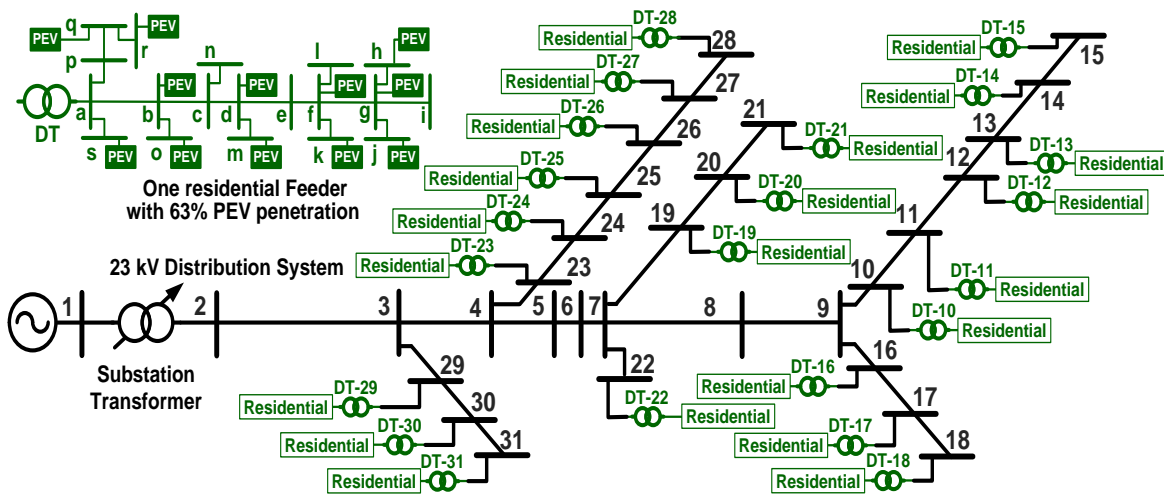**Fig. 3.3. The 449-node smart grid consisting of IEEE 31-node 23kV system and 22 low voltage 19-node 415V residential feeders populated with PEVs [37].**

3.4. Simulation Results without considering Transformer Thermal Limits

Simulations were done on SG of Fig. 3.3 for the six test cases in Table 3.1 for each time slot, $\alpha_{V1}=\alpha_{V2}=0$, $\alpha_D=0.5$ (Eqs. 3.10-3.11) assuming different levels of PEV penetration.

Table.3.1. PEV charging scenarios for the SG system of Fig. 3.3.

Case	Online Charging Approach	Simulations
A	Uncoordinated	Figs. 3.4, 3.8, Table 3.2
B	MSS Coordinated [11]	Table 3.2
C	DPSO Coordinated: (Fig. 3.2(a) without fuzzification)	Figs. 3.5, 3.8, Table 3.2
D	FDPSO Coordinated (Fig. 3.2(a))	Figs. 3.6, 3.8, Table 3.2
E	GA Coordinated (Fig. 3.2(b) without fuzzification and replacing DPSO with GA)	Table 3.2, Figs. 3.8
F	FGA Coordinated (Fig. 3.2(b))	Table 3.2, Figs. 3.7, 3.8

Case A: Uncoordinated PEV Charging

This case was selected to illustrate the impact of charging PEVs at the time of plug-in. Fig. 3.4 and rows 4-10 in Table 3.2 summarise the simulation outcomes, such as the cost of generation, the total power consumed and the losses. To calculate the generation cost for each day, Eq. 3.12 was used.

$$\text{Daily generation cost} = \sum_{m=1}^{288} Generation\, \text{Cos}t\ (m\Delta t) \tag{3.12}$$

According to the results, the distribution transformer was overloaded, and the voltages were no longer within the acceptable range.

Case B: Online MSS Based PEV Charging Algorithm

To compare the quality and accuracy of the results of the proposed algorithms, a sensitivity-based method, as shown in Ref. [37], was used. This case shows that the PEV penetration level was 63% and $SOC_{initial}$ and SOC_{final} were 0% and 100% respectively.
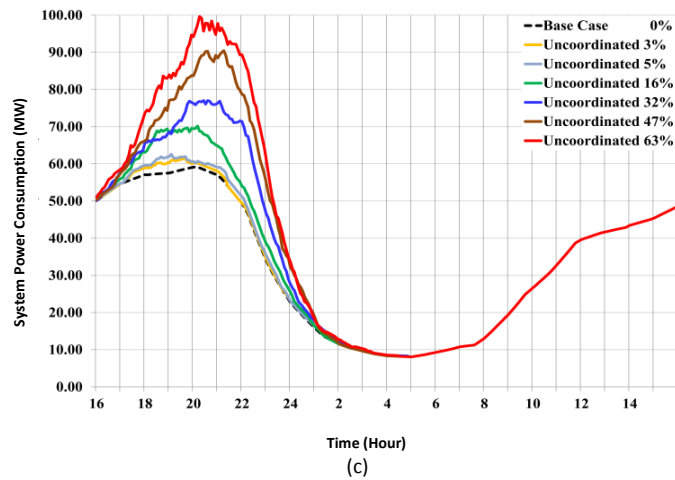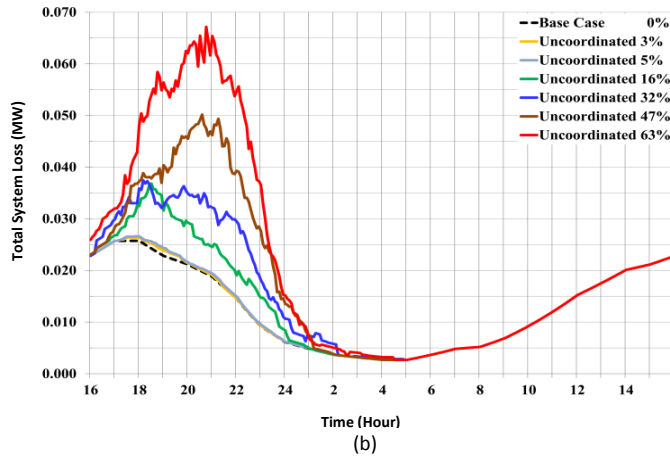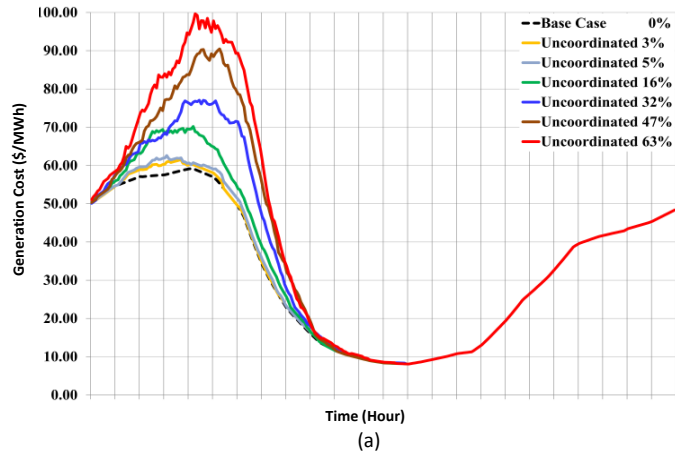
Fig. 3.4. Case A (Table 3.1): simulation results for SG of Fig. 3.3; (a) generation cost, (b) total system losses, (c) system power consumption [57].

Case C: DPSO Coordinated PEV Charging

52

In this case, a discrete PSO algorithm without using the fuzzy system was implemented for PEV charging coordination. Fig. 3.5 and rows 14-18 in Table 3.2 present the simulation results of this case. In this scenario, it can be seen that the overloading in the proposed DPSO, resulted in further losses than Case A and B. Specifically, the cost of generation fell from 100$/MWh (Fig.3.4 (a)) to 69.21$/MWh (Fig. 3.5(a))). The system losses also fell, from 0.67MW in Case A, to 0.034MW. In addition, there was a significant improvement in the cost reduction, when using DPSO when the peak loss period, shifted from 19:00h-22:00h to 24:00h-2:00h.

Case D: FDPSO Coordinated PEV Charging

In this case, the proposed fuzzy system was applied to the DPSO to reach a near global outcome with high performance of the system. Fig. 3.6 and rows 19-25 in Table 3.2 present these optimisation outcomes. It can be seen that the FDPSO prevented an overload of the distribution transformer more rigorously than in Case C. The main reason for this prevention was that the fuzzy system adjusted (reduced) the allowable power transferred through the transformer. Specifically, for a 63% PEV penetration, the allowable power consumption level varied between 0.67MW and 0.86MW, whereas in Case C it was 0.88MW throughout (Figs. 3.5(c) and 3.6(c)).

It should be noted that $D_{fuzzy(t)}$ was adjusted to higher values for early morning hours to make sure all the PEVs in the queue would be charged before 06:00.

A comparison of Figs. 3.5 and 3.6 shows that the application of fuzzy rules offered more reduction in the maximum cost of generation from 69.21$/MWh to 63.18$/MWh. It can also be seen that the maximum total system losses dropped from 0.034MW to 0.032MW and the total daily generation costs reduced from 946.84$/MW to 917.55$/MW.
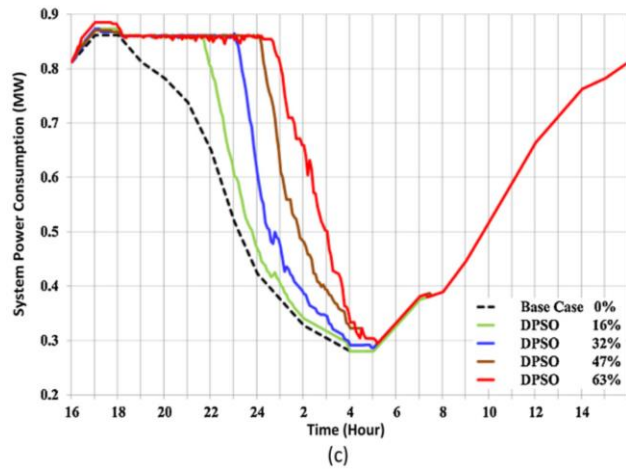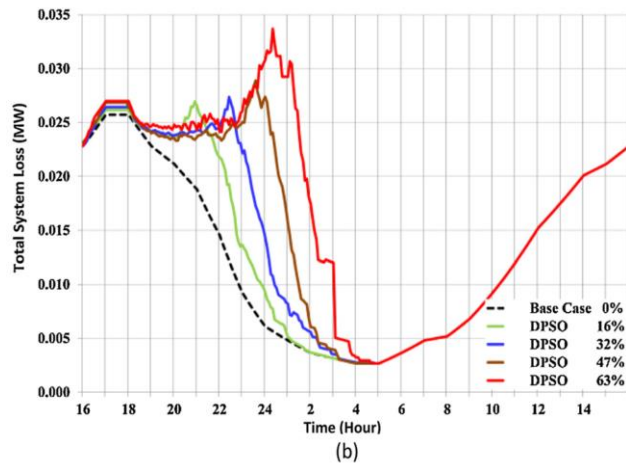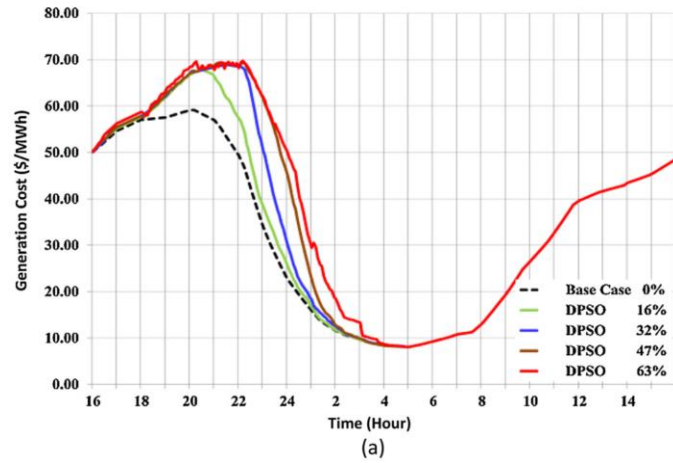
Fig. 3.5. Case C (Table 4.1): simulation results for SG of Fig. 3.3. (a) generation cost, (b) total system losses, (c) system power consumption [57].

54

Cases E-F: GA and FGA Coordinated PEV Charging

More investigation to justify the quality and accuracy of the FDPSO was done by implementing GA and FGA (Fig. 3.2(b)) instead of the PSO and the DPSO. These cases were tested on the same SG network. It can be seen that the results of these two optimisations were very close to those of Cases C and D, and they confirmed the accuracy of the DPSO results (Fig. 3.7 and Table 3.2, rows 26-35). By comparison, the results of the PSO and GA optimisations demonstrate that DPSO and FDPSO are faster and more appropriate for the PEV charging coordination (Table 3.2, last column). The results for FDPSO and MSS charging coordination methods are compared in rows 11-12 of Table 3.2.

(a)

(b)

Fig. 3.6. Case D (Table 3.1): simulation results for SG of Fig. 3.3: (a) generation cost, (b) total system losses, (c) system power consumption [57].

Fig. 3.7. Case F (Table 3.1): simulation results for SG of Fig. 3.3: (a) generation cost, (b) total system losses, (c) system power consumption [57].
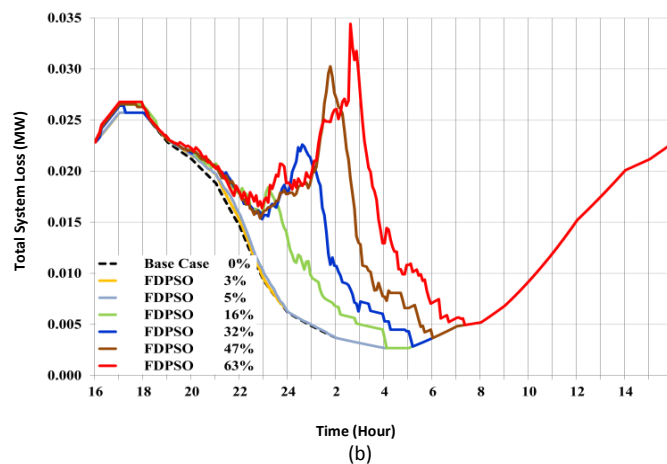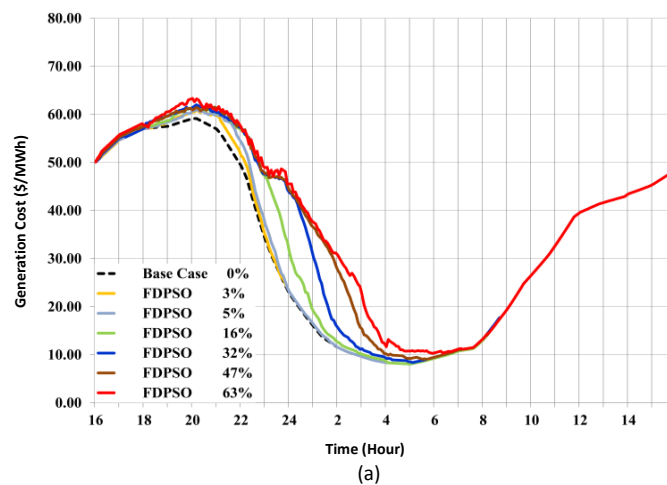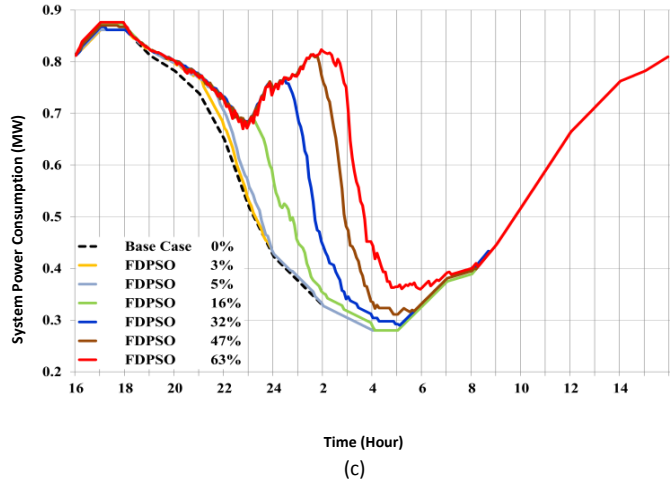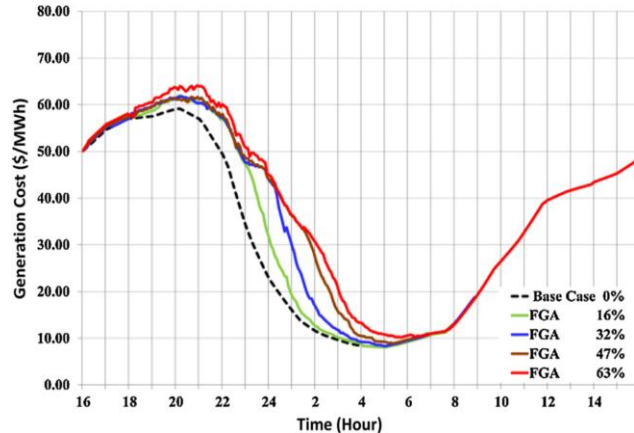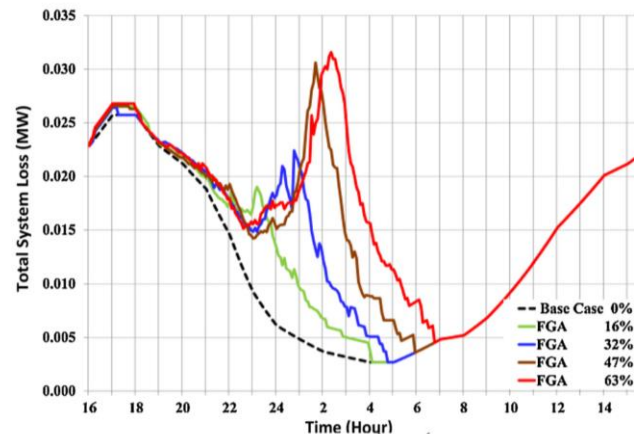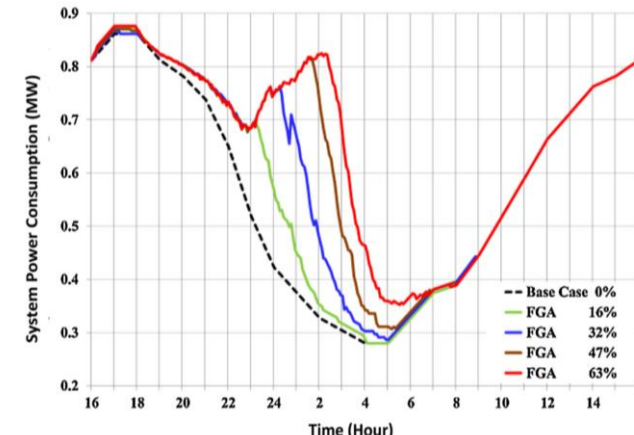
57

Table 3.2. Impact of (un)coordinated PEV charging on the SG of Fig. 3.3.

Row No.	PEV [%]	ΔV [%]*	I MAX [%]**	Total Generation Cost [$/day]	Average Generation Cost [$/MWh] ***	Total Cost [$/day]	Increase in Total Cost [%]	Computing time**** (Sec)
1	Nominal Case: With no PEV (0% PEV penetration)							
2	0	7.63	0	761.51	56.02	776.47	0	NA
3	Case A: Uncoordinated PEV Charging; Figs.3.4, 3.8							
4	3	7.65	2.62	770.40	56.22	785.51	1.16	NA
5	5	7.66	3.64	776.59	56.37	791.79	1.97	NA
6	16	15.11	14.62	827.69	58.20	843.27	8.60	NA
7	32	17.65	15.03	876.09	59.17	893.60	15.08	NA
8	47	19.55	30.69	930.60	60.15	951.25	22.51	NA
9	63	23.40	43.39	978.91	60.95	1004.04	29.31	NA
10	Case B: Comparison between FDPSO (row 11) and MSS (row 12) [11]*****							
11	63	9.86	0.2	859.66	56.11	879.39	11.70	0.033
12	63	10.0	0.172	886	57.83	906	15.04	NA
13	Case C: Online DPSO PEV Coordination; Figs. 3.5, 3.8							
14	16	9.32	0.82	826.06	56.43	841.22	8.34	0.026
15	32	9.38	0.93	867.02	56.86	883.50	13.78	0.028
16	47	9.90	0.99	900.18	58.12	918.59	18.30	0.031
17	63	9.90	2.72	902.35	58.60	946.84	21.94	0.032
18	Case D: Online FDPSO PEV Coordination; Figs. 3.6, 3.8							
19	3	7.63	0.11	768.73	56.11	783.82	0.94	0.026
20	5	7.63	0.12	775.39	56.31	790.55	1.81	0.026
21	16	8.17	0.65	820.40	56.43	835.30	7.57	0.027
22	32	8.42	0.67	851.10	56.59	867.52	11.72	0.029
23	47	9.86	0.99	877.17	56.68	895.25	15.30	0.033
24	63	9.86	1.70	897.88	56.87	917.55	18.17	0.034
25	Case E: Online GA PEV Coordination; Figs. 3.8							
26	16	9.88	0.83	826.16	56.83	841.32	8.35	0.045
27	32	9.90	0.95	866.87	57.64	883.50	13.78	0.047
28	47	10.00	0.99	900.91	58.21	919.41	18.41	0.050
29	63	10.00	2.72	928.24	58.79	948.30	22.13	0.052
30	Case F: Online FGA PEV Coordination; Figs. 3.7, 3.8							
31	16	9.90	0.66	820.40	56.43	835.31	7.58	0.047
32	32	9.90	0.68	851.11	56.59	867.67	11.74	0.048
33	47	9.90	0.99	877.38	56.69	895.43	15.32	0.052
34	63	10.0	1.70	901.57	57.10	921.09	18.62	0.054

*)Average voltage deviation over 24 hours (Eq. 2.6).
**) Increase in transformer current compared with nominal case (no PEVs).
***) Calculated by dividing 'Total Generation Cost in $/day (Table II, column 4)' by 'Total Daily Generation in MWh/day'.
****) Intel Core i5-3570 3.40 GHz processor, 8 GB RAM, using MatLab ver. 8
* ****) In this case, for each PEV, battery size is 8kW, $SOC_{initial}= 0\%$ and $SOC_{initial}= 100\%$.

3.5. Simulation Results considering Transformer thermal Limits

In this section, the objective function proposed above is optimised by taking into consideration the transformer thermal limits.

3.5.1. Transformer Thermal and Aging Modelling

There is a limit to heating in some active parts of transformers, and the greatest concern relates to Hot Spot Temperatures (HST). The HST and transformer life are calculated using IEEE C57.91.1995 [92-94]. To calculate the HST, a thermal model of the 1MVA transformer in Ref [95] is used in this study (Fig.3.8). There are also some details about the thermal model used in Ref [96]. In this chapter $\theta_h = \theta_o + \Delta\theta_h$, where $\Delta\theta_h$ belongs to the HST rises in [^{0}C] and θ_o is used as a top-oil temperature. The balance between the HST and the top-oil temperature was the HST rise found using the following equation:

$$\Delta\theta_{h,r} = H \times g_r$$

where H was the used factor for HST and g_r presents the gradient of the average winding temperature to average oil temperature at full load current.

The total transformer losses were equal to the top-oil temperature rise. The equation below was used to find the top-oil temperature rise [97]:

$$\Delta\theta_o = \Delta\theta_{o,r} \times \left(\frac{P}{P_R}\right)^x = \Delta\theta_{o,r} \times \left(\frac{1+R\times K^2}{1+R}\right)^x \tag{3.13}$$

where P_R was the total loss at rated load in [W], P was the total loss in [W], $\Delta\theta_{o,r}$ was the top-oil temperature rise at rated load in [K], $\Delta\theta_o$ was the top-oil temperature rise in [K], and R was the ratio of load loss to no-load loss at rated load ($K=1$) where K is the current load in [per-unit] or [%].

The following equation (3.14) shows the HST rise above the top-oil temperature (Fig. 3.8):

$$\Delta\theta_h = \Delta\theta_{h,r} \times K^y \tag{3.14}$$

where "y" belongs to the winding exponent. Therefore, the HST will be calculated, as below [97], [98]:

$$\theta_h = \theta_a + \Delta\theta_o + \Delta\theta_h \tag{3.15}$$

where θ_a is the ambient temperature in [^{0}C], and the HST in steady state is found by replacing Eq. 2.2 and 2.3 with Eq. 2.1.

$$\theta_h = \theta_a + \Delta\theta_{o,r} \times \left(\frac{1+R+K^2}{1+R}\right)^x + \Delta\theta_{h,r} \times K^y \tag{3.16}$$

3.5.2 Transformer Loss of Life Calculations

The 'per unit life' (basis for calculating aging acceleration (F_{AA})) based on using the HST would be:

Per unit life= $9.80*10^{-18} e^{\frac{15000}{\theta_h+273}}$ (3.17)

The calculation for aging acceleration (F_{AA}) is:

$$F_{AA} = e^{\left(\frac{15000}{383} - \frac{15000}{\theta_h+273}\right)} \tag{3.18}$$

The equivalent aging (F_{EQA}) is also equal to the following equation:

$$F_{EQA} = \sum_{h=1}^{N} F_{AA,h} \Delta t_h \bigg/ \sum_{h=1}^{N} \Delta t_h \tag{3.19}$$

where h is the time interval and N is the index for the total number of time intervals. The following is the percentage calculation of transformer LOL:
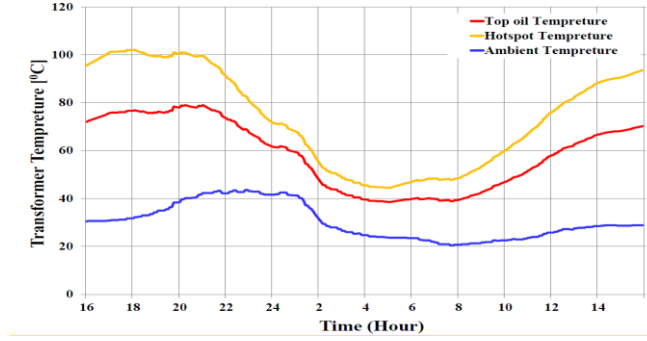
Fig. 3.8. Transformer, ambient, HST and top-oil temperatures

$$\%\text{Loss of Life}= \frac{F_{EQA}*t\times100}{180000} \qquad (3.20)$$

The normal transformer life in this study was 180000 hours. Thus, the simple calculation for LOL

at 120^C for 24 hours, will be 0.1333.

3.5.3. Constraints

The proposed objective function (Eq. (3.1)) was optimised subject to Equations 2.6-2.7, 3.2 and

3.21-3.22.

$$\theta_h \leq \theta_h^{\max} \qquad (3.21)$$

$$\theta_o \leq \theta_o^{\max} \qquad (3.22)$$

In this thesis $\theta_h^{\max}$ =120 [^{0}C], $\theta_o^{\max}$ =85 [^{0}C] (Eqs 3.21-3.22).

3.5.4. Simulation Results

The optimisation for this part was done on a 449-node test system, taking into consideration, the

fact that the thermal limit of the transformer was a new constraint. The results are shown in Fig.

3.9.

61
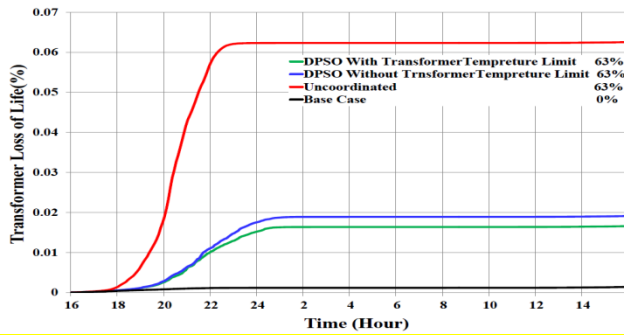
(a)
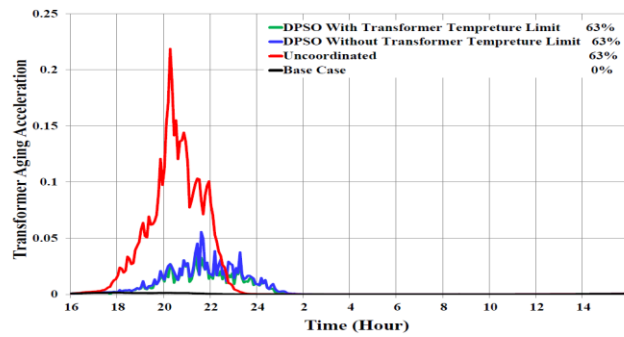
(b)
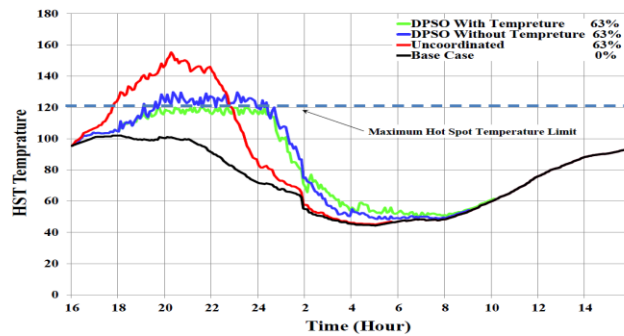
(c)

Fig. 3.9. Simulation results for transformer: (a) LOL variations in a 24 hour period (b) FAA variations in 24 hours, (c) HST variations for four different cases.

3.6. Analysis and Discussion

3.6.1. Voltage Profiles Analysis at Worst Node

The average voltage and the worst node's voltage profiles for 63% PEV penetration, within a 24-hour period for all the cases (A to F) are presented in Fig. 3.10(a). It can be seen that the uncoordinated PEV charging has the lowest voltage profile at the worst node. While, after applying the proposed optimization algorithms, the voltage profile has been very close to the case that there is no PEV in the network (0% PEV). In addition, the worst node voltage profile is less than 0.90pu for all timeslots that the PEVs are being charged. Furthermore, the worst node's voltage is at least 0.90pu in all proposed optimization algorithms and this will satisfy the network constrains. The worst node's voltage profile is also capped at 0.90 when there are significant number of PEVs in the network. The voltage profile gets back to the base profile (0% PEV penetration) after 5:00AM when most of the PEVs have already been charged.

3.6.2. Total Power Consumption for Charging PEVs

The power consumption for implemented cases, including uncoordinated and coordinated PEV charging, is compared in Fig. 3.10(b).

It can be seen that in Case C, based on using Eqs. 3.1-3.2, 2.6-2.7, the PEV charging took place by sending the cost information through the smart meter at each time interval.

It is shown that all the PEVs are being charged by the time of plug-in with uncoordinated case while in the other cases the charging patterns have been postponed to the mid-night.

The peak power consumption time is delayed from around 21:30h to 24:30h to reduce system loading during peak load hours, while its magnitude is increased from 0.34MW to 0.43MW to purchase cheaper energy and reduce $F_{cost\text{-}gen}(t)$. [52-55].

Additionally, using the fuzzy expert system to solve the FGA and FDPSO algorithms to reach near-optimal solutions will cause more delays and change the time of the consumed power to 02:30h.

Moreover, Most PEVs will charge before 06:00h. The last one was at 4:45h, 04:45h, 05:30h and 05:40h for Cases A, C, D and F respectively and there were more cost savings in D and F (Figs. 3.10, Table 3.2).

3.6.3. Random Plug-in Times and PEV Charging Schedules

The number of plugged-in PEVs in all cases with 63% PEV penetration is presented in Fig. 3.10(c). In this figure, the first row is the number of PEVs for Case A (uncoordinated) and the other four rows present the number of PEVs being charged at each time slot for all PEV coordination methods. It can be seen that applying charging coordination methods shifted PEV charging loads to off-peak hours. The SOC variations within the 24 hours are presented in Figs. 4.6(a-d) for the best (DT-20) and the worst (DT-14) feeders.

3.6.4. Computing Times of Proposed Coordination Algorithms

According to Table 3.2, column 7, it can be seen that while the performance of the FDPSO and FGA solutions were close regarding total generation, cost minimisation and voltage profiles, FDPSO was significantly faster than FGA and required 50% less computing time.

3.6.5. Grid performance analysis for low percentage PEV penetration

To be realistic and bearing in mind that PEVs have not yet been fully implemented in public, two different scenarios, with 3 and 5 per cent PEV penetration, were studied. Rows (5-6, 20-21) in

Table 3.2 and Figs. 3.4 and 3.6 present the simulation results for these two scenarios. The results show that with 3% PEV penetration, the maximum power consumption increased to 0.86MW and with 5% PEV penetration to 0.87MW. Furthermore, in the case of the 5% PEV penetration, the maximum generation cost increased from 59$/MWh (no PEV charging) to 63$/MWh (uncoordinated PEV charging). Whereas implementation of the proposed FDPSO sets the maximum generation cost level to 59$/MWh.

(a)

(b)

(c)
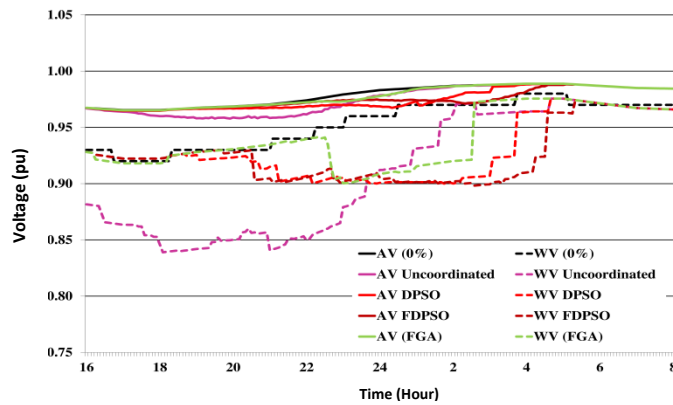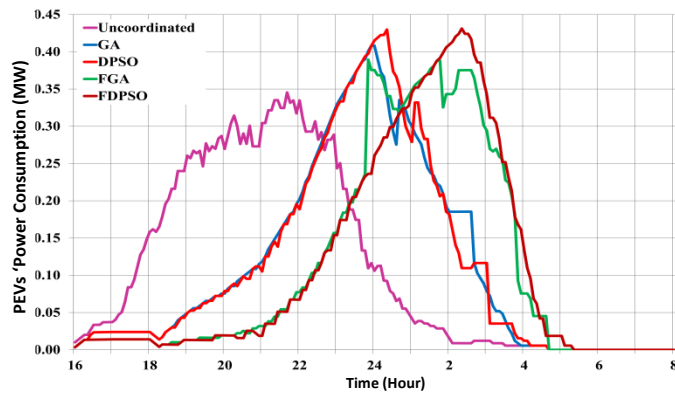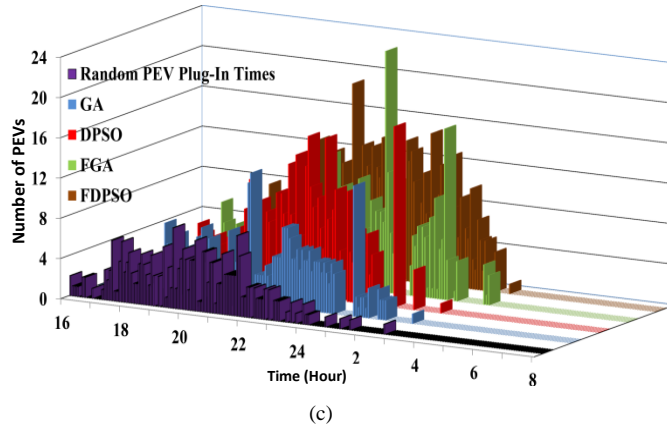
Fig. 3.10. (a) System average voltage (AV) and node worst voltage (WV) profiles for Cases A, C, D and F for 63% PEV penetration. (b) Total power consumption to charge PEVs for Cases A, C, D, E and F with 63% PEV penetration, (c) Random plug-in times (Case A) and coordinated charging schedules for Cases C, D, E and F with 63% PEV penetration [57].

3.7. Summary

According to the simulation results, it is shown that a high PEV penetration level could cause voltage violation and transformer overloading if there is no coordination method.

This chapter proposed two heuristic-based optimisation methods and analysed the results for four different techniques. Detailed simulation outcomes for the test smart grid network are provided and compared with other techniques, including MSS, DPSO and GA for different PEV penetration levels.

The main conclusions can be summarised as follows:

- The proposed FDPSO approach is validated by comparing its solutions with DPSO, GA, FGA algorithms at different PEV penetration levels. It has a superior performance and offers better solutions regarding the total daily generation cost compared to the uncoordinated and the other four coordinated strategies. This superior performance becomes evident when considering the impact of the MEP, the instantaneous DLC, and the number of PEVs in the charging queue.

- While the FDPSO and FGA simulation results are very close, FDPSO is fundamentally faster than GA, which makes it more comfortable for PEV coordination in cases where there is a high level of penetration (Table 3.2, column 7).

- The FDPSO algorithms schedule the charging activities of randomly arriving PEVs at each time slot based on smart meter information. This is done by using online cost minimisation, whilst also taking advantage of the expert knowledge, gained through fuzzy reasoning to postpone some vehicle charging such that the peak power consumption is shifted to the early morning hours to achieve further reductions in total costs and losses.

- Figs. 3.9 shows the simulation results for Loss of Life (LOL) variations in 24-hour. It can be seen that by applying the proposed DPSO algorithm, the LOL drops from 0.062% to less than 0.02%. In addition, the impact of applying DPSO to reduce the aging acceleration and HST, for different cases, is shown in Figs. 3.9 (b, c). The maximum aging acceleration has been changed from 0.22 to 0.051.

- The transformer loss of life for uncoordinated PEV charging is almost three times more than the transformer loss of life resulting from PEV charging coordination (Fig. 3.9(a)).

- The maximum transformer ageing acceleration is 0.22 however after applying DPSO, it is capped at 0.051.

- Fig. 3.9(c) shows that applying DPSO limits the HST while there is 20% of overheating, without any coordination.

CHAPTER FOUR

PEV BATTERY FIXED AND VARIABLE CHARGING SCHEDULING IN THE SMART GRID USING COORDINATED AGGREGATED PARTICLE SWARM OPTIMISATION CONSIDERING CUSTOMER SATISFACTION

In this chapter, a dynamic, online optimisation algorithm using Aggregated Particle Swarm Optimisation (CAPSO) is implemented to achieve an optimal variable charge-rate for each time slot. To maximise and achieve the highest customer satisfaction factor, for each PEV, the proposed algorithm is updated for each time slot (Δt=5min), based on their desired disconnection times, desired state of charges for their batteries and also their acceptance of being charged with a higher electricity price rate.The presented algorithm is subject to the distribution transformers being loaded to their maximum rated capacity, whilst keeping the total grid losses and voltage violations to a minimum.

4.1. Problem Formulation for PEV Charging Coordination

The objective of this chapter is focused on a scenario whereby multiple PEV owners have different preferences and will schedule their charging profiles for time slots of Δt=5min, so as to maximise their customer satisfaction for all PEVs at the next time slot, whilst avoiding grid constraints. Furthermore, this optimisation problem allows for scenarios whereby if a PEV owner chooses to disconnect the PEV earlier than the initially requested departure interval, there will still be an opportunity for the vehicle to receive an acceptable level of state of charge. This is an improvement, compared to the fixed charging-based methods in Refs [32, 36-38, 59-60] where PEVs may not receive any charging services, if they are plugged-out before the designated times. Therefore, the comprehensive objective function of Eq.4.1 is expressed to maximise the total

customer satisfaction by optimising the PEVs' charging rates at each time slot:

$$Max\left(F(t) = \sum_{i=1}^{N_{PEV}} w_i(\Delta t_k)(C_s(\Delta t_{k+1},i) - C_s(\Delta t_k,i)) \right) \tag{4.1}$$

$$for\, i = 1,...,N_{PEV}(\Delta t_k) \quad ,t_k = \Delta t_k, 2\Delta t_k...,24\, hours$$

where

$$w_i(\Delta t_k) = k_1[1 - \frac{SOC(\Delta t_k,i)}{SOC_{Req}(i)}] + k_2[1 - \frac{T_{Remain}(\Delta t_k,i)}{T_{Req}(i)}] + k_3 \frac{Bid(\Delta t_k,i)}{Bid_{Max}(\Delta t_k)} \tag{4.2}$$

$$C_S(\Delta t_k,i) = \frac{SOC(\Delta t_k,i) - SOC_{initial}(i)}{SOC_{Req}(i) - SOC_{initial}(i)} \tag{4.3}$$

In Eq.4.2, $w_i(\Delta t_k)$ is the weighting factor, including the customers' preferences and their

enthusiasm to charge with a higher energy cost at the time slot (Δt_k). For instance, there may be a

case in which the PEV owner is willing to pay more than the normal price and the PEV has a low

SOC and also needs to depart quickly. In this case, the above formulations provide a higher

weighting factor in the optimisation problem.

To calculate SOC for the next time slot $SOC(\Delta t_{k+1},i)$, there are different techniques presented in Refs

[99-103].This thesis adopts the battery equivalent circuit model of Ref [99], consisting of a

resistance, which is in series with a voltage source, as shown in Fig.4.1 (b). This model is

represented as:

$$V_i(\Delta t_k) = V_{oc,i} + R_i I(\Delta t_k,i) \tag{4.4}$$

$$I(\Delta t_k,i) = CR_i^{best}(\Delta t_k,i) \times I^{Rated}(i) \tag{4.5}$$

The $SOC(\Delta t_{k+1},i)$ can be formulated based on the charging current as follows:

$$SOC(\Delta t_{k+1},i) = SOC(\Delta t_k,i) + (\frac{\Delta t}{Q_i} I(\Delta t_k,i) \times \Upsilon) \times 100 \tag{4.6}$$

where, Υ is the status of each PEV where digits '1' and '0' correspond to the PEV being

connected or not connected. The power delivered to PEV during the charging process is:

$$P_{PEV}^{Delivered}(\Delta t_k,i) = V_{oc}(i) \times I(\Delta t_k,i) + R_i I^2(\Delta t_k,i)$$
$$= V_{oc}(i) \times CR_i^{best}(\Delta t_k,i) \times I^{Rated}(i) + R_i(CR_i^{best}(\Delta t_k,i) \times I^{Rated}(i))^2$$
(4.7A)

Moreover, the power consumed by the ith PEV from the grid considering the impact of charger's efficiency (Fig.4.1 (a)) is:

$$P_{PEV}^{Consumed}(\Delta t_k,i) = P_{PEV}^{Delivered}(\Delta t_k,i) / \eta_{ch}(CR_i(\Delta t_k))$$
(4.7B)

$$P_{PEV}^{Consumed}(\Delta t_k,i) \times \eta_{ch}(CR_i(\Delta t_k)) = V_{oc}(i) \times CR_i^{best}(\Delta t_k,i) \times I^{Rated}(i) + R_i(CR_i^{best}(\Delta t_k,i) \times I^{Rated}(i))^2$$
(4.7C)

The charging current can be calculated from (4.7A), as follows:

$$I(\Delta t_k,i) = \frac{\sqrt{4 \times \Delta t \times R_i \times P_{PEV}^{Consumed}(\Delta t_k,i) \times \eta_{ch}(CR_i^{best}(\Delta t_k)) + V_{oc,i}^2} - V_{oc,i}}{2R_i \times CR_i^{best}(\Delta t_k,i)}$$
(4.8)

Substituting Eq.4.8 into Eq.4.6 yields:

$$SOC(\Delta t_{k+1},i) = SOC(\Delta t_k,i) + \left(\frac{\Delta t \times \sqrt{4 \times \Delta t \times R_i \times P_{PEV}^{Consumed}(\Delta t_k,i) \times \eta_{ch}(CR_i^{best}(\Delta t_k)) + V_{oc,i}^2} - V_{oc,i}}{2R_i \times CR_i^{best}(\Delta t_k,i) \times Qi} \times \Upsilon \right) \times 100$$
(4.9)

A numerical example for the calculation of SOC (based on Eqs. 4.6-4.9) is provided in the Appendix A.

Appendix A: Numerical Example for Calculation of SOC

This appendix presents a numerical example for the calculation of SOC based on Eqs. 4.6-4.9. Assuming the battery bank voltage is 400V, the battery capacity is 10kWh, and the nominal cell voltage for lithium ion batteries is 3.2V, then the number of cells for the whole battery bank will be 125. It is also considered that the internal resistance for each cell is 2mΩ and then the total battery bank resistance is R_i= 2mΩ×125=250mΩ. In this thesis, each time slot is assumed to be 5 minutes; therefore Δt =1/12=0.0833 hours. To calculate Q_i, the battery capacity (10KW) should be divided by its open circuit voltage (400V); therefore, Q_i=10,000/400=25Ah. Detailed calculations of SOC using Q_i are presented in Table 4.1.

In the Coulomb counting technique, the charges flowing into and out of the battery are integrated so as to gain an accurate estimate of the remaining capacity and calculation of the SOC [105]. This technique uses a shunt to measure battery current, and a coulomb counting circuit which is effectively a very accurate current-integrating Analog to Digital Converter (ADC) technique. Following this, the measured battery voltage and current are sent to a microprocessor, whereby the microprocessor contains battery chemistry specific information, such as cell impedance, within its memory. To communicate with the rest of the system a standard protocol such as I^2C communication can be used. Subsequently, the SOC is calculated using Eqs. 4.6-4.9.

Practically, for the real-time calculation of the battery SOC, at each time slot (Δt =5 minutes), the following steps, should be taken.

1- The battery ampere hour rate is calculated as Qi= (Battery Capacity)/V_{oc}.

2- Measuring open circuit voltages of the PEV batteries (V_{oc}).

3- Measuring the battery current using a shunt.

4- Sent the measured battery voltage and current to the microprocessor using a standard protocol such as I^2C communication.

5- Using Equation (4.7-4.9) to calculate SOC.

Note that if the battery is connected to a charger with CR=0.3, then the required time (without considering losses) to fully charge the battery is 1/0.3=3.333 hours. If one considers the impacts of the losses, then the battery will only be charged to 86% of its rated capacity. Therefore, more time will be required to fully charge the battery if the losses are included.

Table 4.1. Calculation of SOC

Input Data to Calculate SOC	
V_{oc} for the battery bank (V)	400
R_i for the battery bank (ohm)	125×0.002=0.25
Charger efficiency at CR^{Best} based on Fig 4.1(a)	0.93
CR^{best} which is a sample of results for *ith* PEV achieved by CAPSO	0.30
Nominal charger capacity $P_{consumed}$ (W)	10000
Δt	0.083
$SOC_{Initial}$ (%)	0
Rated battery ampere hour Qi (Ah)	10000÷400=25
Calculations	
I_i^{Rated} (considering losses) (A)	6.450
I_i^{Rated} (not considering losses) (A)	7.5
Increment of SOC for the Next 5 Minutes Using Eq.4.9	
Increment of SOC for the next 5 minutes (considering losses) (%)	2.150
Increment of SOC for the next 5 minutes (not considering losses) (%)	2.5
SOC After the Nominal Charge Time of 1/0.3=3.333 Hours with CR=0.3	
SOC after 3.333 hours (considering losses) (%)	86.0
SOC after 3.333 hours (not considering losses) (%)	100

4.2. Assumptions and Definitions

• PEVs can be connected/disconnected at any time according to the customer's needs. Customers will input their requested plug-out times and requested final SOCs, at the time of plug-in. In this thesis, it is considered that all the PEVs will be charged at PEV owners' location.

• Compared to the short term Market Energy Price (MEP, Fig 2.1), there will be some customers who will be prepared to pay a higher rate, for their special charging requirements.

• Each hour is divided into 12 time slots of $\Delta t=5$ minutes. The reason to choose the 5-minute time interval is to provide acceptable time duration for the PEV chargers to transfer reasonable amount of energy to the batteries. For example, if a PEV charger is rated at 5kW, then the amount of power used in one minute is about 80W (=5000/60). If the battery size is 10kWh, then 80W/min

will increase the SOC by 0.83% per time slot (assuming that a PEV has been selected for charging). Even if we accept less than 1% charge per minute, in practice this is not realistic, as the number of switches for the chargers will be much higher than the acceptable range.

- During each time slot, the aggregator is expected to have the existing charging power. Each PEV can be charged after plug-in, with a variable charge-rate at each time slot and is expected to reach the desired SOC_{Req}, by the requested plug-out time.

- The aggregator has access to the PEV information using smart metering technology including their locations, charger types, battery sizes, and plug-in time.

- At each time slot, the status of each PEV will be updated. This is not a given parameter and each PEV will send a plug-in signal, when it is being randomly connected to the grid.

- Fig. 4.2(a) shows the spectrums of the random plug-in times and requested plug-out times of the PEVs.

- A PEV-Queue Table will be generated to keep track of the vehicles' status including their plugged-in times; requested and actual plugged-out times; initial SOCs; requested and actual SOCs; charger type and battery sizes. As a result, after plugging a new PEV at Δt_k, the Table will be updated, and the implemented CAPSO coordination algorithm will be executed to obtain a new optimal online charging schedule.

- PEV chargers are controllable and have variable charging functions. During the charging process, each PEV is presumed to have a variable active load.

- The requested time $T_{Req}(i)$, for each PEV must be greater than the minimum charging time $T_{min}(i)$, required to charge the battery which depends on the maximum charge-rate allowed. where,

$$T_{\min}(i) = \frac{SOC_{\text{Req}}(i)\text{-}SOC_{initial}(i)}{Charger_{Size}(i)}$$

(4.10)

- The proposed coordination process is updated when a new vehicle is plugged-in, or an existing one plugs out, or a time slot has passed periodically.

- To improve customer satisfaction, PEVs are allowed to be disconnected before their requested plug-out times. This will considerably complicate the coordination algorithm.

(a)

(b)
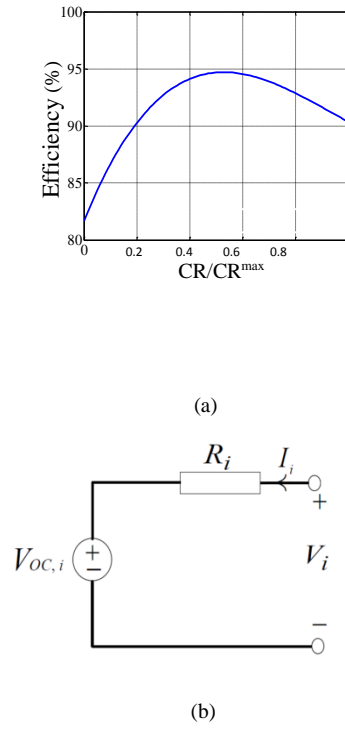
Fig.4.1. Modeling of PEV battery [38]; (a) typical charger efficiency (CR corresponds to charging efficiencies), (b) equivalent circuit [104].

4.3. Constraints

In this chapter the following equations are used as constraints to supply the base and PEV loads:

$$V_{\min} \leq V_j(\Delta t_k) \leq V_{\max}, \quad \text{for} \quad j = 1,...,N_{node}$$

(4.11)

$$D_t(\Delta t_k) = \sum_{k=1}^{n} P_k(\Delta t_k) = \sum_{k=1}^{n} (P_{load_k}(\Delta t_k) + P_{PEV,i}(\Delta t_k)) \leq D_{\max}(\Delta t_k)$$

(4.12)

$$D_{\max}(\Delta t_k) = Max\{DL(\Delta t_1), DL(\Delta t_2),...,DL(\Delta t_k)\}, \kappa = 1,...,288 \tag{4.13}$$

To sustain battery health, its SOC level should be conserved to within the range recommended by the manufacturer. Therefore, the following SOC constraint is included:

$$SOC_{initial}(i) \le SOC(\Delta t_k, i) \le SOC_{Req}(i), for\, i = 1,...,N_{PEV}(\Delta t_k) \tag{4.14}$$

Once SOC $(\Delta t_k, i)$ reaches $SOC_{Req}(i)$, the ith battery charger will be switched to standby mode.

C presents the rate of charge or discharge of the battery which is based the total size (capacity Ah) of the battery. In this thesis, the variable charging rates are considered to be from $0C$ to $CR_i^{\max} = 1C$ whilst, 10% of vehicles are assumed to have fast charging facilities with charge rates of up to $CR_i^{max} = 2C$. A random generator is used to generate the charge-rates. The PEV charge-rates will be controlled as follows:

$$0 \le CR_i \le CR_i^{\max} \quad CR_i \in \Re \quad i = 1,...,N_{PEV}(\Delta t_k) \tag{4.15}$$

4.4. Simulation input data

The continuous uniform random number generator is used to simulate the random plug-in times and expected plug-out times (Fig. 5.2(a)), as well as the requested SOCs. The initial State Of Charge $SOC_{initial}$ (%) for each PEV is calculated upon the basis of its trip length, as follows (Eq. 5.16) [88]:

$$SOC_{initial} = \begin{cases} \alpha_i - (\alpha_i - \beta_i) \times \dfrac{L_j}{L_i^{max}} & for\ \ L_j \le L_i^{max} \\ \beta_i & otherwise \end{cases} \tag{4.16}$$

$$for\, i = 1,...,N_{type\, of\, PEVs}, j = 1,...,N_{PEV}(\Delta t_k)$$

where i indicates the type of PEVs, j is the number of PEVs.
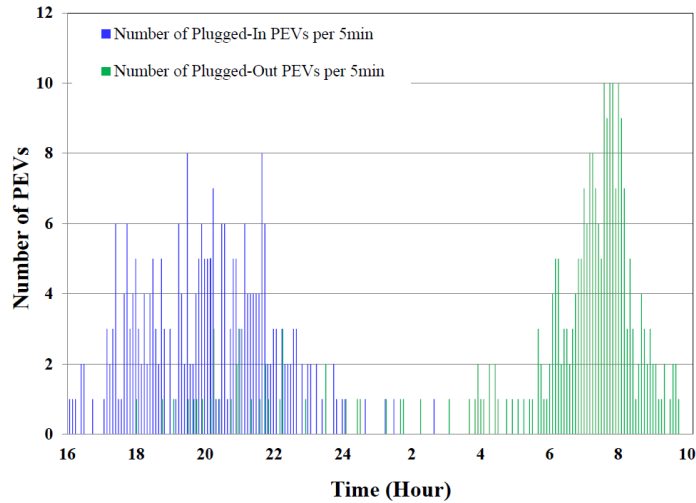
(a)
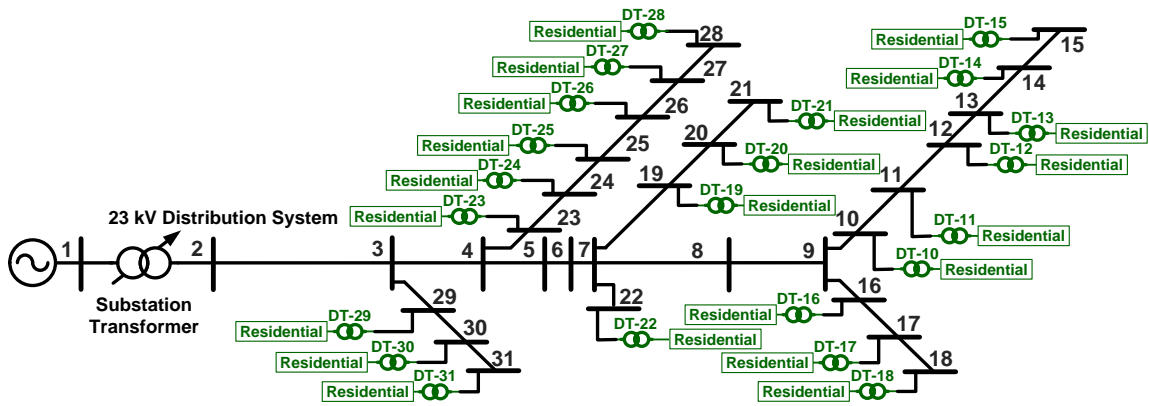
(b)
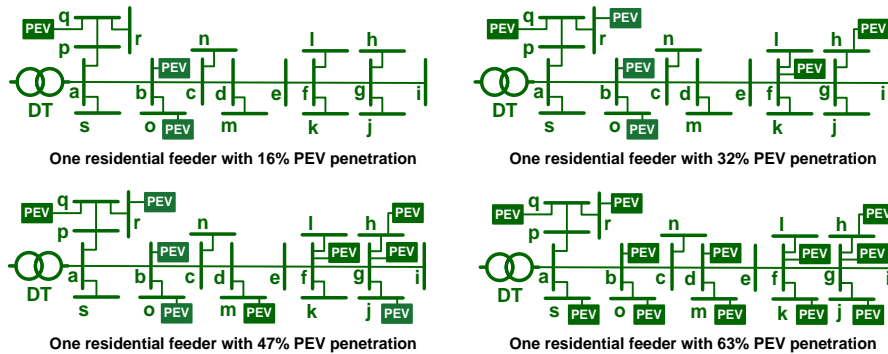
(c)

Fig. 4.2. System characteristics: (a) spectrums of the random plug-in times and the requested plug-out times of the simulated PEVs, (b) the 449 node SG consisting of IEEE 31-node 23kV system and 22 low voltage 19-node 415V residential feeders populated with PEVs [16], (c) detailed diagram of one residential feeder in Fig. 5.2(b) with 16%, 32%, 47% and 63% PEV penetration [104].

4.5. Implemented Online PEV charging coordination Algorithm

The CAPSO algorithm has been used to solve different optimisation problems [76]. In CAPSO, each particle updates its position, by considering the positions of particles that have performed better. Thus, this thesis applies the CAPSO algorithm to identify the best solutions to the PEV coordination problem (Eqs4.1-4.15). The established CAPSO algorithm, in this thesis, updates the velocity vector using the same technique presented in Ref [93].

4.5.1. Proposed Initial Population and Structure of Particles:

The selected particles for variable charge-rate online PEV coordination contain the charging rates $CR_i(\Delta t_k)$ for each PEV at Δt_k, that are restricted to between 0 and 2C, as follows (Eq.4.17):

$$\begin{cases} \overbrace{\begin{pmatrix} CR_1(\Delta t_k) & CR_2(\Delta t_k) & \dots & CR_{N_{PEV}}(\Delta t_k) \\ CR_1(\Delta t_k) & CR_2(\Delta t_k) & \cdots & CR_{N_{PEV}}(\Delta t_k) \\ \vdots & \vdots & \vdots & \vdots \\ CR_1(\Delta t_k) & CR_2(\Delta t_k) & \dots & CR_{N_{PEV}}(\Delta t_k) \end{pmatrix}} \end{cases} \tag{4.17}$$

4.5.2. CAPSO Fitness Function

To improve quality of CAPSO solutions, fitness functions are used to reach this objective within the identified constraints (Eqs.4.1-4.15). The inverse algebraic products (Eq.4.18), of the proposed penalty functions for voltage (Eqs.4.19-4.20) and demand (Eq.4.21) are used as the fitness function, to combine the PEV coordination objective function (Eq.4.1) and constraints (Eqs.4.11-4.15):

$$F_{fitness}(\Delta t_k) = \frac{F(\Delta t_k)}{F_V(\Delta t_k) \times F_D(\Delta t_k)} \tag{4.18}$$

$$F_V(\Delta t_k) = \prod_{k=1}^{n} F_{V,k}(\Delta t_k) \tag{4.19}$$

$$F_{V,k}(t) = \begin{cases} e^{\alpha_{V_1}(1-V_k(t))} & V_k(t) \leq V_{min} \\ 1 & V_{min} \leq V_k(t) \leq V_{max} \\ e^{\alpha_{V_2}(V_k(t)-1)} & V_k(t) \geq V_{max} \end{cases}$$

(4.20)

$$F_D(\Delta t_k) = \begin{cases} 1, & D_t(\Delta t_k) \leq D_{max}(\Delta t_k) \\ e^{\alpha_D(D_t(\Delta t_k)-D_{max}(\Delta t_k))}, & D_t(\Delta t_k) \geq D_{max}(\Delta t_k) \end{cases}$$

(4.21)

4.5.3. Simulation Results

To present the effectiveness of the proposed algorithm and the impacts of considering variable charging, simulations are accomplished on the SG of Fig. 4.2(b) for the three cases of uncoordinated and CAPSO-based coordinated PEV charging, with FCC and VCC, using a time interval of Δt =5 minutes; PEV penetration levels of 0% (no PEVs), 16%, 32%, 47% and 63% (Fig. 4.2(c)) considering N_{bus}=449, N_{line}=448, W=0.73, C1=2.05, C2=2.05, and N_{pop} = 100, α_{V1}=α_{V2}=0.3 and α_D=0.5 (Eqs.4.19-4.20). Simulation results are shown in Figs. 4.3-4.6 and Tables 4.2, 4.3.

To compare the performance of FCC and VCC schemes, detailed simulations will also be presented for the three selected feeders in Fig. 4.2(b) with the best (DT-20), moderate (DT-12) and worst (DT-14) performances. The first feeder receives 100% of customer satisfaction, with both FCC and VCC; the second feeder receives 100% of customer satisfaction, with VCC and the third feeder doses not receive 100% customer satisfaction, regardless of the selected (FCC or VCC) coordination approach. It should be noted that DT-20 and DT-12 are not the only feeders that receive 100% of customer satisfaction with VCC. The complete lists of best feeders are DT-9, DT-13, DT-20 and DT-22, whereas the complete lists of the moderate feeders are DT-3, DT-4, DT-5, DT-7, DT-11, DT-12, DT-18 and DT-21.

In this thesis, the backward-forward sweep method is used to calculate the power (load) flows and bus voltages. It is assumed that the generation capacity is large enough to supply both the base and the PEV charging loads in all time slots.

At each time slot ($\Delta t=5$ minutes), the weakest bus is defined to be the bus with the lowest voltage magnitude. The locations and voltage magnitudes of the weak buses will change within the 24 hours depending on the system base load the system configuration and the PEV loadings (numbers, locations, random plug-in times and charging rates of the activated PEVs). To identify the weakest bus at each time slot, the optimal PEV coordination is performed, the selected PEVs are activated, power flow calculation is performed, nodes are sorted based on their voltage magnitudes, and the weakest node is the one that has the minimum voltage amongst all other nodes. This process is repeated for 24-hours, to generate the weak voltage profiles of Figs. 4.3(c), 4.4(c) and 4.5(c).

Case A: Uncoordinated PEV Charging

The impact of Uncoordinated PEV Charging is investigated by starting the charging process as soon as vehicles are randomly plugged in. Simulation results are shown in Table 4.2 (rows 4-8) and Fig.4.3. As expected, the SG is facing overloading, voltage regulation and efficiency problems. For example, for 63% PEV penetration, maximum power consumption has increased by about 45% (Fig.4.3 (b)) compared to the nominal operation with no vehicles. Also, the minimum voltage for 63% of PEVs penetration has decreased by 30%, compared to its nominal value, as shown in Fig.4.3(c). Moreover, in this case, there is about 10% voltage violation for 32% PEV penetration. Furthermore, it has been demonstrated that the voltage drops to 0.7p.u. (Fig.4.3(c)), thus, in reality it may cause system collapse and should be limited by the system operator. To

overcome problems associated with uncoordinated PEV charging, the CAPSO algorithm of Section IV is adopted.
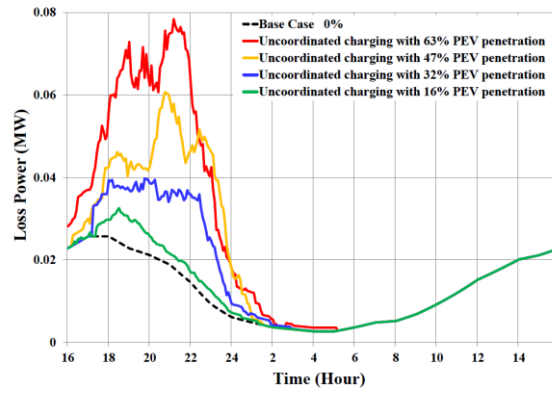
(a)
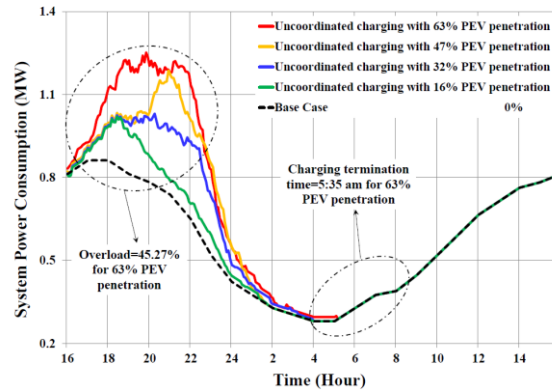
(b)
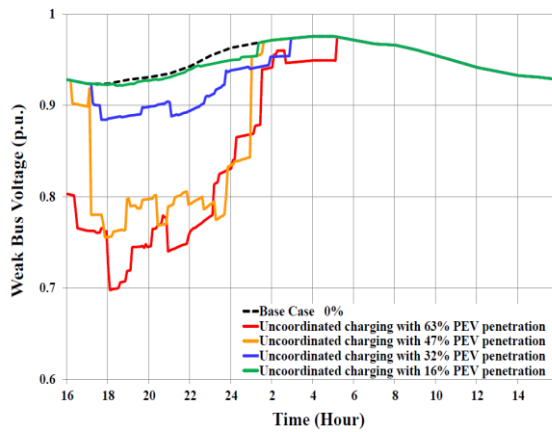
(c)

Fig. 4.3. Simulation results for Case A with 16, 32, 47 and 63 percent of PEV penetration: (a) loss of power, (b) system power consumption, (c) weak bus voltage [104].

Case B: Coordinated PEV Charging using CAPSO with FCC

In this approach, the charging process of each PEV is realised at a fixed charge rate, corresponding to the nominal charging rate of its charger. In detail, the charging process of each user starts by receiving a charging signal from the charging centre and will be connected until it receives its required State Of Charge. The implemented CAPSO algorithm is used for optimal PEV charging coordination with a fixed nominal charging rate. While PEV will be automatically disconnected, when reaching their requested SOC levels, the consumers can also disconnect their vehicles prior to the requested plug-out times. Simulation results for FCC are presented in Fig.4.4 and Table 4.2 (rows 9-13). Compared to Case A, FCC is offering further improvements in substation transformer loading, power losses and weak bus voltages. However, it is important to note that, the overloading, of the main substation transformer, still remains a concern.

(a)

(b)

(c)

Fig. 4.4. Simulation results for Case B with 16, 32, 47 and 63 percent of PEV penetration: (a) loss of power, (b) system power consumption, (c) weak bus voltage [104].

Case C: Coordinated PEV Charging using CAPSO with VCC

Simulation results including system power consumptions and loss using the CAPSO algorithm with the variable charge-rate strategy are shown in Fig.4.5 and Table 4.2 (r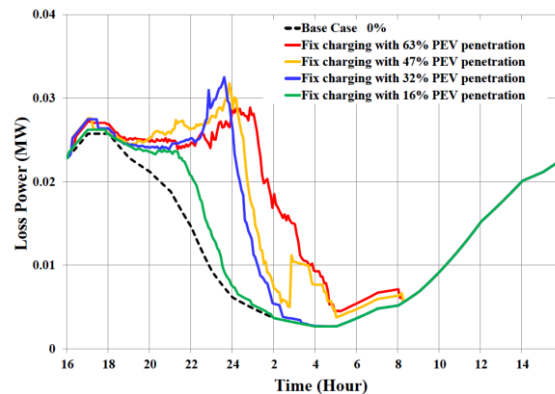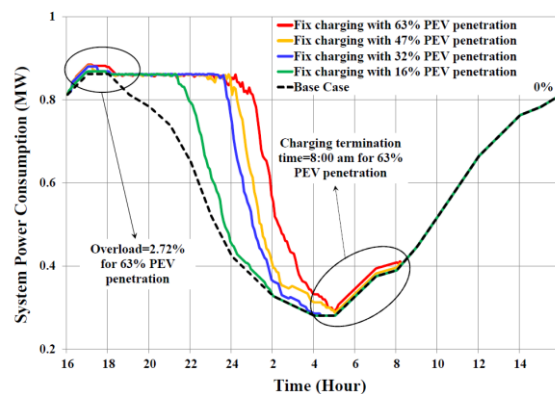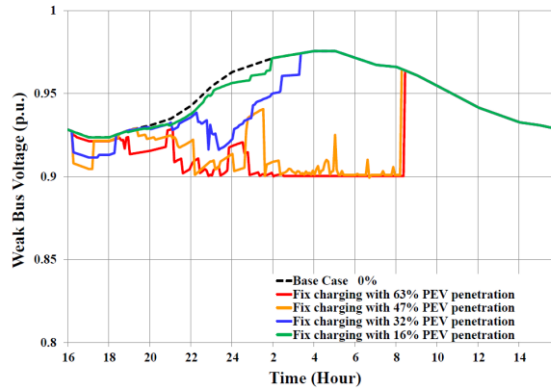ows 14-18). Compared to Case B, VCC, more strictly prevents system (transformer) overloading (Fig.4.5 (b)). It can be observed that for 63% PEV penetration, VCC has the advantage of completing the charging process for all vehicles sooner than the FCC. However, for lower PEV penetration levels of 47%, 32% and 16%, the two charging strategies have similar characteristics. In addition, there is no overloading in the systems power consumption when using the VCC. This is because it is limited to the designated 0.84MW. In comparison, there is about 2.72% overloading in the substation transformer using FCC (Fig.4.4 (b)). Moreover, the voltages are in their permissible limit, and there is no problem with the voltage profiles (Fig.4.5(c)).

According to Fig. 4.4(a), it can be seen that applying CAPSO postpone the load to the off peak and the power losses will remain almost the same as base case (0% PEV penetration). However, if the PEV penetration is increased, then the power losses will also increase to 0.033MW.

Moreover, according to Fig. 4.4(b), the system power consumption is remained at 0.084MW, using CAPSO and there is no overload, even with 63% PEV penetration.

Furthermore, almost all PEVs were charged before 05:00h and the rest received the required charge by 08:00h.

Also in Fig. 4.4(c), the CAPSO had a significant impact on improving the weak bus voltage profile and the voltage for the weak bus is above 0.9pu, for all time slots.

Comparing the results of the CAPSO, using FCC (Figs. 4.4) and VCC (Figs. 4.5) demonstrates that by applying CAPSO and using VCC:

- The maximum loss of power has decreased from 0.033MW to 0.0315MW.

- There is no overload in Fig 4.5. (b), However in Fig. 4.4(b), there is a slight overloading of the main transformer between the hours of 17:00h to 18:00h.

- All the PEVs were charged before 06:00h, where in Fig. 4.5(b), there are few PEVS that received charge after 06:00h.

- The average of the weak bus voltages, using VCC, is actually better than FCC.

Table 4.2. Impact of PEV charging on the SG of Fig. 4.2(b).

PEV [%]	ΔV* [%]	IMAX [%]**	Customer Satisfaction	Computing time*** (Sec)
Nominal Case: With no PEV				
0	7.63	0	NA	NA
Case A: Uncoordinated PEV Charging; Fig. 4.3				
16	10.08	18.42	NA	NA
32	12.60	19.58	NA	NA
47	25.10	37.62	NA	NA
63	31.00	45.27	NA	NA
Online PEV Coordination (DPSO) with FCC (Ref. [27])				
16	9.32	0.82	NA	0.026
32	9.38	0.93	NA	0.028
47	9.90	0.99	NA	0.031
63	9.90	2.72	NA	0.032
Case B: Online PEV Coordination (CAPSO) with FCC; Fig.4.4				
16	9.42	1.39	98.37	0.027
32	9.53	2.03	95.57	0.028
47	9.91	2.09	90.54	0.032
63	9.94	2.72	88.38	0.034
Case C: Online PEV Coordination (CAPSO) with VCC; Fig.4.5				
16	9.06	0.00	99.09	0.028
32	9.16	0.00	96.91	0.029
47	9.58	0.00	94.47	0.034
63	9.73	0.00	93.89	0.035

*) Average voltage deviation over 24 hours.
**) Increase in transformer current compared with the nominal case (no PEVs).
***) Intel Core i5-3570 3.40 GHz processor, 8 GB RAM, using MATLAB ver. 8

4.6. Discussion and Analysis

The SOC variations within the 24 hours are presented in Figs. 4.6(a-d) for the best (DT-20) and the worst (DT-14) feeders:

• Figures 4.6(a) and 4.6(b) present the profiles for the state of charge variations for all the PEVs for two different charging coordination algorithms. It can be seen that in Fig 4.6(a) there is a significant difference between the starting times for the first and the last PEVs. It is also shown that the first PEV starts charging at 20:15PM and the last one does not have a chance to start earlier than 3:45AM. To prevent this and optimize the customer satisfaction function, the proposed variable charging algorithm has been applied to charge all the PEVs as soon as the system constrains are satisfied.

- The charging patterns for this case are shown in Fig 4.6(b). According to this figure, all the PEVs are being charged around 21:00PM and the charging process finishes at 3:05AM.

- Comparing figures 4.6(a) and 4.6(b) shows that the PEVs with VCC received the required SOC one hour earlier than the case with FCC. If the PEV owners at nodes "l" and "j" unplug their PEVs earlier than mid-night, then there will be no charge for them using FCC. However, all the PEVs received minimum 40% of their required SOC using VCC method.

- Figures 4.6(c) and 4.6(d) present the profiles for the state of charge variations for all the PEVs for two different charging coordination algorithms. In these figures, it is shown that some of the PEVs may not be charged at the worst branch using FCC method.

- In Fig 4.6(c), similar to the figures 4.6(a) and 4.6(b), there is a significant difference between the starting times for the first and the last PEVs.

- According to Fig.4.6(c) with FCC, at the worst feeder, there were 4 out of 12 PEVs, that were not charged at all, and their initial SOCs, were also not changed. Therefore, the customer satisfaction at these nodes, was zero, thus indicating a reduced overall, satisfaction level at this feeder (DT-14). The detailed results are presented in Figures 4.6(e) and 4.6(f).

- The results of VCC pattern are shown in Fig 4.6(d). According to this figure, all the PEVs are being charged at 18:00PM and the charging process finishes at 2:20AM. It is shown that all PEVs received at least 20% of the required SOC and there is no PEV with no charge using variable charging method.

It is depicted that with FCC the first and the last PEV start charging times in feeder DT-1, were at 19:00 and 04:00, respectively; whilst with the VCC (Fig.4.6(d)), some of the PEVs had started charging as early as 17:50 , and the last vehicle had been activated at 19:20 on node 's'.
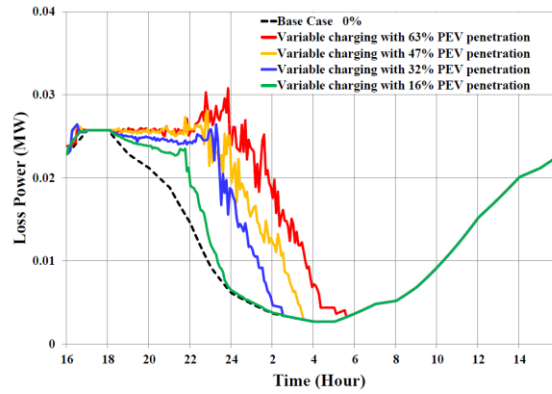
(a)
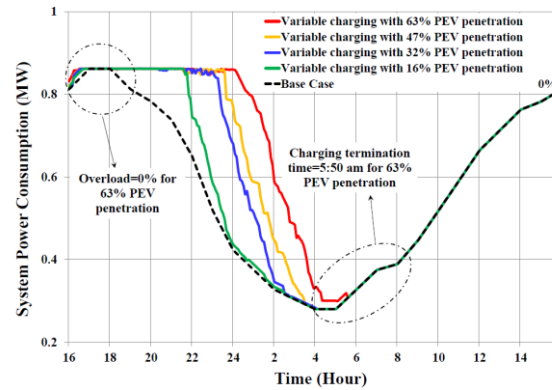
(b)
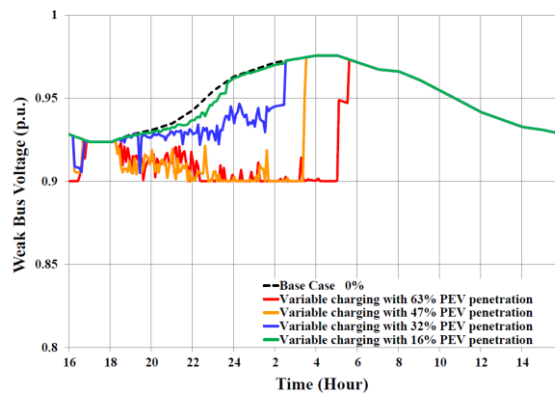
(c)

Fig. 4.5. Simulation results for Case C with 16, 32, 47 and 63 percent of PEV penetration: (a) loss of power, (b) system power consumption, (c) weak bus voltage [104].

• The VCC strategy is capable of fully or partially charging the PEVs that were not scheduled with

FCC (e.g., were not allowed to start charging). For example, with the FCC, the PEVs located on

nodes b, d, f and h of feeder DT-14 had nil customer satisfaction levels (Fig.4.6(f)) whilst, with

86

the VCC their customer satisfaction rates improved by 100%, 23.85%, 35.94% and 23.70%, respectively.

• Comparison between Figs.4.6(a, b) shows that all PEVs in the best feeder (DT-20) reach their requested SOCs before their requested plug-out times whilst using VCC and all vehicles are charged by 03:40.

With FCC the PEV on node 'l' is not activated and has not received the charging service until 03:35. However with the VCC strategy, the same vehicle at the same time will be fully satisfied and receive 100% of its requested SOC. The bar charts of Fig.4.6 (e, f) and Table 4.3 show the level of customer satisfaction for the best and worst feeders:

• Using FCC, the customer satisfaction for four of the PEVs was nil, whereas when using VCC all vehicles received full or partial charging; Table 4.3 (rows 9-10, 18-19, and 27-28). Figs.4.6 (g, h) indicate the customer satisfaction profiles for all feeders (DT-1 to DT-22) using VCC and FCC strategies:

• The numbers of feeders that reached 100% customer satisfaction using VCC and FCC approaches, were 12 and 4, whilst according to Table 4.3 (rows 9-10) the minimum levels of customer satisfactions in the worst feeder (DT-14) are 78% and 64%, respectively.

• The feeders had reached their requested SOC at the same time as the VCC (Fig. 4.6(h)). However with the FCC, there was a significant time difference in obtaining the requested SOC, even for the fully satisfied customers (Fig. 4.6(g)). For instance, feeder DT-12, reached 100% customer satisfaction at time slot 110, whilst feeders DT-8 and DT-9 received 100% of customer satisfaction at time slot 130.

(a)

(b)

(c)

(d)

(e)

(f)
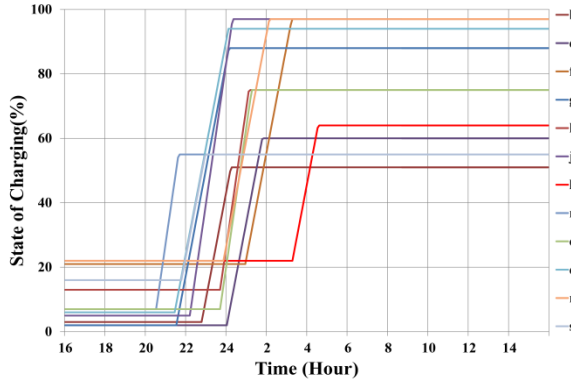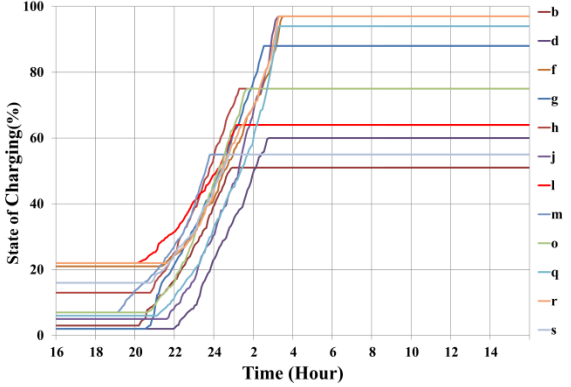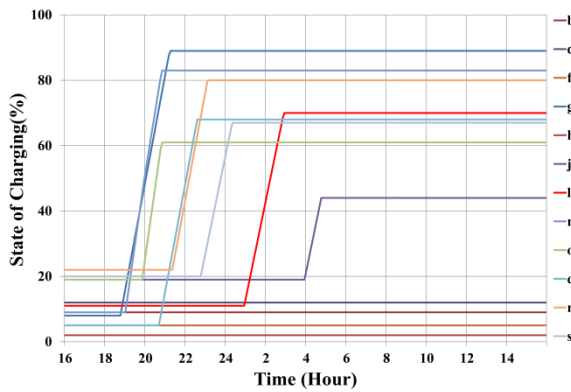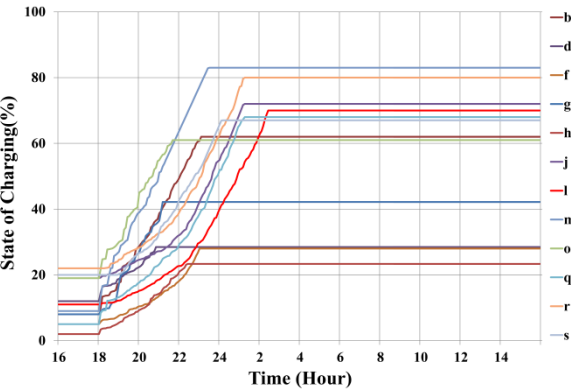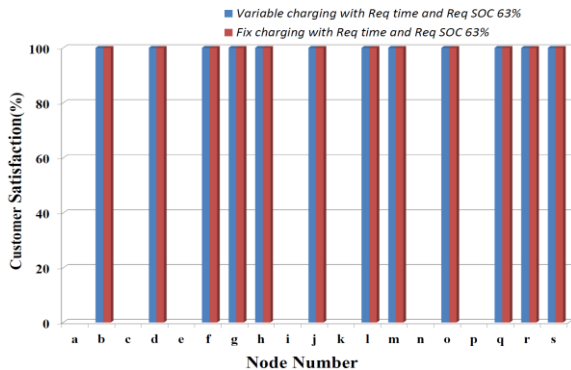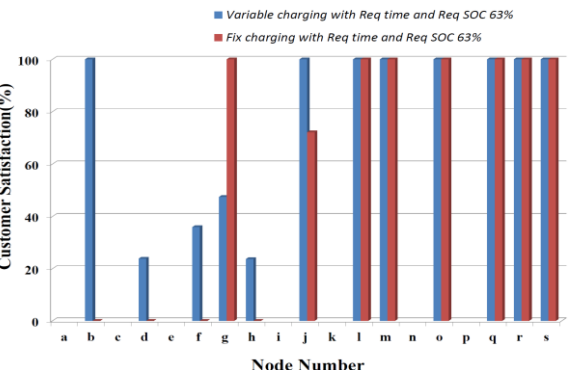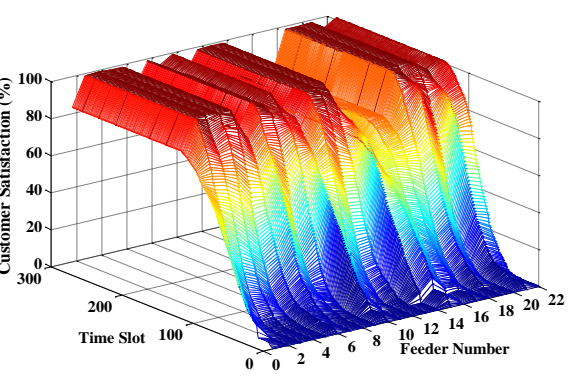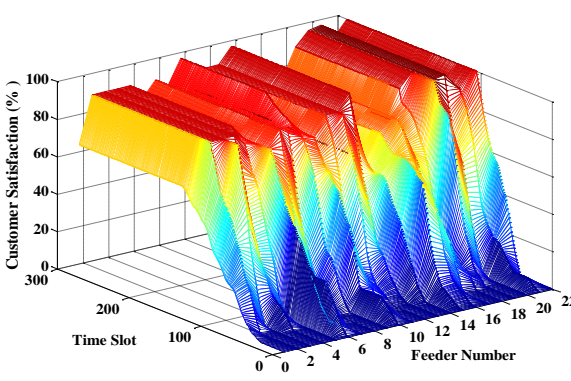
Fig.4.6. (a) Sample battery SOCs of feeders in Fig.4.2(c) for best feeder (DT-20) using FCC, Fig.4.6. (b) Sample battery SOCs of feeders in Fig.4.2(c) for best feeder (DT-20) using VCC, Fig.4.6. (c) Sample battery SOCs of feeders in Fig.4.2(c) for worst feeder (DT-14) using FCC, Fig.4.6. (d) Sample battery SOCs of feeders in Fig.4.2(c) for worst feeder (DT-14) using VCC, Fig.4.6. (e) Customer satisfaction of few feeders in Fig.4.2(c) using FCC and VCC for best feeder (DT-20), Fig.4.6. (f) Customer satisfaction of few feeders in Fig.4.2(c) using FCC and VCC for worst feeder (DT-14), Fig.4.6. (g) Customer satisfaction profiles for all feeders (DT-1 to DT-22) in Fig.4.2(c) using FCC, Fig.4.6. (h) Customer satisfaction profiles for all feeders (DT-1 to DT-22) in Fig.4.2(c) using VCC [104].

4.7. Summary

This thesis has implemented an online variable charge-rate PEV coordination approach, using CAPSO, to maximise the total level of customer satisfaction. The proposed VCC approach will also minimise the grid losses without exceeding the grid constraints. This is subject to the requested plug-out times form the customers, desired state of charges (SOC_{Req}) for each PEV and the PEV owners' willingness to be charged   a higher rate at each time slot, so as to receive more power.

Detailed simulation results for a 449-node SG network have been presented, compared and analysed for uncoordinated PEV charging and coordinated PEV charging using FCC and VCC strategies. The main conclusions are:

• The proposed coordinated charging algorithm takes into consideration the random plug-in times, initial SOCs, requested plug-out times and the requested final SOCs, as well as the maximum battery charging rates, battery and charger efficiencies.

• With the VCC, customer's satisfaction level was high. In comparison, when using FCC, some vehicles may not even start charging before their requested plug-out times.

• The substation transformer is not overloaded when utilising the VCC option, whilst overloading conditions are noticed with the FCC even at low levels of PEV penetrations of 16% and 32%.

• The VCC strategy is capable of fully or partially charging the PEVs. In comparison that were not scheduled with the FCC.

• There was no overload in system power consumption when using the VCC, as it is limited to the designated 0.84MW, however there was about 2.72% overloading, in the substation transformer whilst using the FCC .

Table.4.3. Detailed simulation results for coordinated (CAPSO) PEV charging of Fig. 4.2(b) for worst, moderate and best feeders using FCC and VCC.

Node Number		b	D	f	g	h	j	l	M	o	q	r	s	Ave.
For the Worst Feeder (DT-14)														
Plug-in Time Slot		21	14	20	15	19	24	25	21	21	23	28	36	22
Initial SOC [%]		9	12	5	8	2	19	11	9	19	5	22	20	11
Requested Plug-Out Time Slot		103	58	84	62	77	151	157	104	112	145	167	175	116
Request SOC [%]		62	92	99	89	82	72	70	83	61	68	80	67	77
Actual SOC at T_{Req} for VCC [%]		62	22	36	42	19	72	70	83	61	68	80	67	57
Actual SOC at T_{Req} for FCC [%]		0	0	0	89	0	52	70	83	61	68	80	67	487
Consumer Satisfaction (Eq.4.3) [%]	VCC	100	24	36	48	24	100	100	100	100	100	100	100	78
	FCC	0	0	0	100	0	72	100	100	100	100	100	100	64
For the Moderate Feeder (DT-12)														
Plug-in Time Slot		73	83	46	42	55	54	63	42	61	68	51	50	57
Initial SOC [%]		26	7	12	23	18	28	4	28	7	17	27	20	18
Requested Plug-Out Time Slot		198	205	184	181	189	188	192	181	192	194	187	186	189
Request SOC [%]		84	59	73	94	97	64	93	65	68	66	53	57	72
Actual SOC at T_{Req} for VCC [%]		84	59	73	94	97	64	93	65	68	66	53	57	72
Actual SOC at T_{Req} for FCC [%]		84	59	73	94	97	29	93	65	68	66	53	57	69
Consumer Satisfaction (Eq.4.3) [%]	VCC	100	100	100	100	100	100	100	100	100	100	100	100	100
	FCC	100	100	100	100	100	0	100	100	100	100	100	100	91
For the Best Feeder (DT-20)														
Plug-in Time Slot		76	61	36	51	64	83	38	85	114	49	68	46	64
Initial SOC [%]		9	24	7	3	28	26	16	12	8	21	21	28	16
Requested Plug-Out Time Slot		201	192	176	188	193	205	178	207	216	185	195	184	193
Request SOC [%]		58	84	74	76	76	57	55	60	52	74	58	56	65
Actual SOC at T_{Req} for VCC [%]		58	84	74	76	76	57	55	60	52	74	58	56	65
Actual SOC at T_{Req} for FCC [%]		58	84	74	76	76	57	55	60	52	74	58	56	65
Consumer Satisfaction (Eq.4.3) [%]	VCC	100	100	100	100	100	100	100	100	100	100	100	100	100
	FCC	100	100	100	100	100	100	100	100	100	100	100	100	100

CHAPTER FIVE

SUMMARY AND CONCLUSIONS

In the research for this thesis, the optimal PEV charging coordination to maximise all customers' satisfaction without exceeding grid constraints was performed. For the FCC, the VCC and the uncoordinated charging of PEVs, the simulation results were compared on a 449-node test system using CAPSO. The proposed algorithms take into consideration the random plug-in times, initial SOCs, requested plug-out times, requested final SOCs and the maximum charging rates of the PEV batteries.

To compare the performance of the proposed optimization methods, four algorithms are tested and implemented:

- ➢ A heuristic-based Online Coordinated Charging Genetic Algorithm (OL-CC-GA) is implemented for the charging of PEV batteries in the SG. This minimises the cost related to the system losses and the generated energy. It also increases the number of charged PEVs, adjusting the node voltage and diminishes the load for the distributed transformer. OL-CC-GA, also considers the changing of the distribution transformer loading for online and delayed (e.g., full-overnight and partial-overnight) PEV charging.

- ➢ Implementation of two different algorithms (FGA and FDPSO) for PEV charging coordination. These two decreases the cost related to the generated energy and system losses. They also increase the amount of delivered power to PEVs and regulate the node voltages.

- ➢ The proposed and optimised algorithm uses CAPSO to solve the variable PEVs charging problem. The time interval used for this algorithm is Δt=5min. It is used

91

to maximise the customers' satisfaction levels for all PEV owners, based on their requested plug-out times, requested battery state of charges (SOC_{Req}) and willingness to pay the higher charging energy prices. The algorithm also ensures that the distribution transformer is not overloaded whilst grid losses and node voltage deviations are minimised over the 24 hour period.

In summary, the presented methods for PEV charging coordination are based on the below steps:

Step 1: Predication and forecasting the based DLC for all of the feeders

It is assumed that there is no PEV load on the DLC, and the information in DLC includes active and reactive powers for all of the feeders. It should be noted that if daily forecasted data without PEV penetrations are available, there is no need to perform this step.

Step 2: Load Modelling

Each load at each feeder is being modelled as a variable PQ load and changes according to the forecasted LDC of the first step.

Step 3: Reading information for each PEV

In this step, information such as location, state of charge and requested charged time should be provided to the algorithm as an input data.

Step 4: Fuzzy technique implementation

According to the above information, as well as the forecasted energy price for each interval, fuzzy output (Transformer limit) should be extracted.

Step 5: Optimisation technique execution

To apply any of the proposed optimisation methods, a random generator should be used to generate an initial population based on the available data for each PEV. Next, all of the constraints should be implemented and the fitness function(s), evaluated. Subsequently, the optimisation operators

should be applied to generate a new population, unless the stopping criteria have been reached. It should be noted that Step 5 should be conducted at each new time interval.

Step 6: Update the DLC and repeat Step 5

The current DLC is to be updated according to the optimal charging rates for the PEVs, and then the Step 5 will apply. This process is online and dynamic, and is to be repeated for all 288 (5-minute) time intervals throughout the day.

5.1. Research Conclusions

The main conclusions of this research are as follows:

- Customers received higher levels of satisfaction while using the VCC strategy. Comparatively, when using the FCC, some vehicles may not even start charging before their requested plug-out times.

- The substation transformer is not overloaded when using the VCC option, whilst overloading conditions are noticed with the FCC strategy, even with low levels of PEV penetrations of 16% and 32%.

- The VCC strategy is capable of fully or partial charging the PEVs that were not even scheduled with the FCC option.

- Equality in the SOC distribution is ensured in the proposed charging pattern (VCC) at each time slot for all PEVs. Then, there will be a reasonable state of charge, in case the PEV owner leaves before his/her initially scheduled departure time.

- Amongst the implemented GA, FGA, DPSO and FDPSO optimisation methods, for different PEV penetration levels, the FDPSO offers the best solution among the other used algorithms according to the total daily generation cost.

- Two implemented algorithms (FDPSO and FGA) are very similar, but the optimisation speed for FDPSO is faster than FGA. Therefore, it is more suitable to use in online PEV scheduling (Table 4.3, column 7), and also more suitable for online PEV coordination of large SG configurations.

- The FDPSO scheme used the FES to postpone some of the PEVs' charging and shift their charging time to the early morning hours, due to having fewer total losses and costs.

- The implemented OL-CC-GA schedules the charging activities of randomly arriving PEVs at each time slot based on smart meter information using online cost minimisation. The modified OL-CC-GA, takes advantage of the expert knowledge, to vary the distribution transformer loading level ($D_{max}(t)$ in Eq.2.12) and perform delayed PEV charging. It does so by postponing some vehicle charging, such that the peak power consumption is shifted to the early morning hours to achieve further reductions in the total costs as compared to the online coordination strategy.

- In OL-CC-GA, the total system cost has the maximum value amongst the three cases B, C and D; however, all PEVs will be charged before 06:00. Also, case B has the maximum losses amongst all coordinated cases, whilst the generation cost has the minimum value in case D compared with the other cases.

- In delayed partial-overnight PEV charging coordination, the generation cost is higher than case D and less than case B.

5.2. Future Work

Future works, which are related to this study, will be considered as follows:

1- Implementation parallel optimisation tools:

The charging coordination problem is an online optimisation problem and the calculation time is an important factor. Applying parallel optimisation tools may reduce the computation burden and achieve better results.

2- Dynamic load modelling:

As the behaviour of the loads depends on various parameters and the value of the DLC for each time interval, is a crucial factor in these optimisation approaches, dynamic modelling of the load may provide precise results.

3- Unbalanced variable PEV charging coordination:

In the real world, most of the distribution systems are unbalanced, and each PEV has a chance to connect to any of the phases, which may cause more problems within the system.

4- Dynamic load forecasting:

In this thesis, it is assumed that the DLC has been forecasted one day ahead, where if dynamic load forecasting techniques apply; there will be a chance to get better results.

5- Using decentralised charging coordination methods

To reduce the communication burden, optimal decentralised control approaches are suggested.

6- Optimal locating and sizing D-FACTS

Recently the Distributed flexible AC transmission devices have become more popular. It is suggested that the PEV charging coordination problem, be solved simultaneously with optimal locating and sizing of the D-FACTS.

7- Incorporation of Wind and Solar generation systems

These days, wind farm and PV systems are connected to most of the distribution systems. Therefore, the PEV charging coordination problems will provide more realistic outcomes. It would

be more convincing, if an online forecasting tool applies to have an accurate prediction of the output of the wind/solar system.

8- Charging Coordination considering G2V, V2G and V2V simultaneously

In this thesis, it is only considered that the PEVs are being charged from the grid, whereas there is some research performed on V2G. The optimisation which considering the combination of G2V, V2G and V2V in a system, is another area that requires more research.

REFERENCES

[1] M. Yilmaz, P.T. Krein ," Review of Battery Charger Topologies, Charging Power Levels, and Infrastructure for Plug-In Electric and Hybrid Vehicles ," IEEE Transaction on power electronics, Vol. 28, No. 5, 2013.

[2] A.S. Masoum, S. Deilami, P.S. Moses, A.Abu-Siada, "Impacts of Battery Charging Rates of Plug-in Electric Vehicle on Smart Grid Distribution Systems," Innovative Smart Grid Technologies Conference Europe, 2010.

[3] M. Bertoluzzo, N.Zabihi, G.Buja, "Overview on Battery Chargers for Plug-in Electric Vehicles," International Power Electronics and Motion Control Conference, 2012.

[4] T.Krein,"Intelligent Battery Management for Maximum Performance in Plug-In Electric and Hybrid Vehicles, "IEEE Vehicle Power and Propulsion Conference, 2007.

[5] S. Lacroix, E. Laboure, M. Hilairet, "An Integrated Fast Battery Charger for Electric Vehicle," Vehicle Power and Propulsion Conference, 2010.

[6] H. Bai,Y. Zhang,C. Semanson, C. Luo, C.C. Mi, , "Modelling, design and Optimisation of a Battery Charger for Plug-in Hybrid Electric Vehicles ," IET Electrical Systems in Transportation, 2010.

[7] E. A,Rezai , M. F. Shaaban , E. F. El-Saadany , A. Zidan, " Uncoordinated Charging Impacts of Electric Vehicles on Electric Distribution Grids: Normal and Fast Charging Comparison " , Power and Energy Society General Meeting, 2012.

[8] A. S. Masoum, A. Abu-Siada, S. Islam, "Impact of Uncoordinated and Coordinated Charging of Plug-In Electric Vehicles on Substation Transformer in Smart Grid with Charging Stations," Innovative Smart Grid Technologies Asia, 2011.

[9] P. S. Moses, M.A. S. Masoum, S. Hajforoosh, "Overloading of Distribution Transformers in Smart Grid Due to Uncoordinated Charging of Plug-In Electric Vehicles," Innovative Smart Grid Technologies (ISGT), 2012.

[10] F.Jiyuan and S. Borlase, "The Evolution of Distribution," IEEE Power and Energy Magazine, Vol. 7, No. 2, pp. 63-68, 2009.

[11] K. Clement-Nyns, E. Haesen, and J. Driesen, "The Impact of Charging Plug-in Hybrid Eectric Vehicles on a Residential Distribution Grid," IEEE Transactions on Power Systems, Vol. 25, No. 1, pp. 371-380, 2010.

[12] C. Jamroen, P. Namproom, S. Dechanupaprittha, "TS-Fuzzy Based Adaptive PEVs Charging Control for Smart Grid Frequency Stabilization," Procedia Computer Science, Vol. 86, pp. 124-127, 2016.

[13] Z. Xu, Z. Hu, Y. Song, Z. Luo, K. Zhan, J. Wu, "Coordinated Charging Strategy for PEVs Charging Stations," IEEE Conference on Power and Energy Society General Meeting, 2012.

[14] G. Li, X.P. Zhang, "Modeling of Plug-in Hybrid Electric Vehicle Charging Demand in Probabilistic Power Flow Calculations", pp. 492 – 499, 2012.

[15] L.P. Fernan´dez, T. Román, R. Cossent, C.M. Domingo, P. Frías, "Assessment of the Impact of Plug-in Electric Vehicles on Distribution Networks," IEEE Transaction on Power System, Vol. 26, No. 1, pp. 206–213, 2011.

[16] M.G. Vayá, L.B. Roselló, G.Andersson, "Optimal Bidding of Plug-in Electric Vehicles in a Market-Based Control Setup", Power Systems Computation Conference (PSCC), 2014.

[17] Han, S., Han, S., and Sezaki, K. (2010). Development of an optimal vehicle-to-grid aggregator for frequency regulation. Smart Grid, IEEE Transactions on, 1(1), 65−72.]

[18] Sundstrom, O. and Binding, C. (2010). Planning electricdrive vehicle charging under constrained grid conditions. In Power System Technology (POWERCON), 2010 International Conference on, 1–6. IEEE.

[19] Lee, K.Y.; El-Sharkawi, M.A. Modern Heuristic Optimization Techniques Theory and Applications to Power Systems, 1st ed.; Wiley: Hoboken, NJ, USA, 2008.

[20] 40. Amaris, H.; Alonso, M.; Alvarez-Ortega, C. Reactive Power Management of Power Networks

with Wind Generation, 1st ed.; Springer: Berlin, Germany, 2013

[21] S. Shao, T. Zhang, M. Pipattanasomporn, R. Saifur, "Impact of TOU Rates on Distribution Load Shapes in a Smart Grid with PHEV Penetration," IEEE PES Transmission and Distribution Conference, pp.1–6, 2010.

[22] K. Qian, C. Zhou, M. Allan, Y. Yuan, "Modeling of Load Demand due to EV Battery Charging in Distribution Systems," IEEE Transaction on Power System, Vol. 26, No. 2, pp. 802–810, 2011.

[23] W. Su, M.Y. Chow, "Investigating a large-scale PHEV/PEV Parking Deck in a Smart Grid Environment," 43rd North American Power Symposium, 2011.

[24] W. Su, M.-Y. Chow, "Sensitivity Analysis on Battery Modeling to Large-scale HEV/PEV Charging Algorithms," 37th Annual Conference IEEE Industrial Electronics Society, pp. 7–10, 2011.

[25] W. Su, M.-Y. Chow, "Evaluation on Intelligent Energy Management System for PHEVs Using Monte Carlo Method", Electric Utility Deregulation and Restructuring Conference, pp. 1675–1680, 2011.

[26] C. Roe, J. Meisel, A. P. Meliopoulos, F. Evangelos, T. Overbye, "Power system level Impacts of PHEVs," 42nd International Conference on System Sciences, pp. 1–10, 2009.

[27] K. J. Dyke, N. Schofield, M. Barnes, "The Impact of Transport Electrification on Electrical Networks," IEEE Transaction on Industrial Electronics, Vol. 57, No. 12, pp. 3917–3926, 2010.

[28] S. Shojaabadi, S. Abapour, M. Abapour, A. Nahavandi, "Optimal Planning of Plug-in hybrid Electric Vehicle Charging Station in Distribution Network Considering Demand Response Programs and Uncertainties", IET Generation, Transmission & Distribution, Vol.10, No.13, 2016.

[29] P. Palensky and D. Dietrich, "Demand side management: Demand response, intelligent energy systems, and smart loads," IEEE Transaction on Industrial Informatics, Vol. 7, No. 2, pp. 1551–3203, 2011.

[30] W. Su, M.-Y. Chow, "Performance evaluation of a PHEV Parking Station Using Particle Swarm Optimization," IEEE Power Energy Society General Meeting, 2011, pp. 1–6.

[31] W. Su, M.-Y. Chow, "Performance Evaluation of an EDA-based large-scale Plug-in Hybrid Electric Vehicle Charging Algorithm," IEEE Transaction on Smart Grid, Vol. PP, No. 99, 2011.

[32] C.K. Wen, J.C. Chen, J.H. Teng, P. Ting, "Decentralized Plug-in Electric Vehicle Charging Selection Algorithm in Power Systems," IEEE Transaction on Smart Grid, Vol. 3, No. 4, pp. 1779-1789, 2012.

[33] M. D. Galus, G. Andersson, "Demand Management of Grid Connected Plug-in Hybrid electric Vehicles (PHEV)," IEEE Energy 2030 Conference, pp. 1-8, 2008.

[34] C. Hutson, G.K. Venayagamoorthy, K.A. Corzine, "Intelligent Scheduling of Hybrid and Electric Vehicle Storage Capacity in a Parking lot for Profit Maximization in Grid Power Transaction Actions", IEEE Energy Conference, pp. 1–8, 2008.

[35] W. Su, H. Rahimi-Eichi, W. Zeng, M.Y. Chow, "A Survey on the Electrification of Transportation in a Smart Grid Environment", IEEE Transaction on Power Systems, Vol.3, No.1, pp.1-10, 2012.

[36] K. Clement-Nyns, E. Haesen, J. Driesen, "The Impact of Vehicle-to-grid on the Distribution Grid", Electric Power Systems Research, Vol.81, No.1, pp.185-192, 2011.

[37] S. Deilami, A.S. Masoum, P.S. Moses, M.A.S. Masoum, "Real-time Coordination of Plug-in Electric Vehicle Charging in Smart grids to Minimize Power Losses and Improve Voltage Profile", IEEE Transaction on Smart Grid, Vol.2, No.3, pp.456-467, 2011.

[38] M.F. Shaaban, M. Ismail, E.F. El-Saadany, W. Zhuang, "Real-time PEV Charging/discharging Coordination in Smart Distribution Systems," IEEE Transaction on Smart Grid, Vol.5, No.4, pp.1797-1807, 2015.

[39] E. Sortomme, M. M. Hindi, S. D. J. MacPherson and S. S. Venkata, "Coordinated Charging of Plug-in Hybrid Electric Vehicles to Minimize Distribution System Losses", IEEE Transaction on Smart Grid, vol.2, No.1, pp. 198- 205, 2011.

[40] R. Mehta, D. Srinivasan, A. Trivedi, "Optimal Charging Scheduling of plug-in Electric Vehicles for Maximizing Penetration within a Workplace Car Park", Evolutionary Computation (CEC), 2016.

[41] J. Tomic, W. Kempton, "Using Fleets of Electric-drive Vehicles for Grid Support," Journal of Power Sources, Vol. 168, No. 2, pp. 459 – 468, 2007.

[42] S. B. Peterson, J. Whitacre, J. Apt, "The Economics of Using Plug-in Hybrid Electric Vehicle Battery Packs for Grid Storage," Journal of Power Sources, Vol. 195, No. 8, pp. 2377- 2384, 2010.

[43] S.L. Andersson, A. Elofsson, M. Galus, L. G¨oransson, S. Karlsson, F. Johnsson, G. Andersson, "Plug-in Hybrid Electric Vehicles as Regulating Power Providers: Case studies of Sweden and Germany," Energy Policy, Vol. 38, No. 6, pp. 2751 – 2762, 2010.

[44] P. Richardson, D. Flynn, A. Keane, "Local Versus Centralized Charging Strategies for Electric Vehicles in Low Voltage Distribution Systems," IEEE Transaction on Smart Grid, Vol. 3, pp. 1020-1028, 2012.

[45] I. Jiang, Y. Fei, "Decentralized scheduling of PEV on-street Parking and Charging for Smart Grid Reactive Power Compensation", Innovative Smart Grid Technologies (ISGT), 2013.

[46] D. Beyer, S. Ruhe, P. Bretschneider, J. Ehrhardt, "Results of a Monte Carlo Based Risk Analysis on the Impact of PEVs to the Distribution Grid," IEEE International Energy Conference (ENERGYCON), 2016.

[47] D. Dallinger, J. Link, M. Buttner, "Smart Grid Agent: Plug-in Electric Vehicle", IEEE Transactions on Sustainable Energy, Vol.5, No.3, 2014.

[48] A. Ahuja, S. Das, A. Pahwa, "An AIS-ACO hybrid approach for Multi-objective Distribution System Reconfiguration," IEEE Transactions on Power Systems, Vol. 22, No. 3, pp. 1101 –1111, 2007.

[49] D. Steen, T.L. Anh, M.O. Vasquez, O. Carlson, L. Bertling, V. Neimane, "Scheduling Charging of Electric Vehicles for Optimal Distribution Systems Planning and Operation," in CIRED, pp. 1 – 4, 2011.

[50] J. Villar, C.A. Díaz, J. Arnau, F. A. Campos, "Impact of Plug-in-Electric Vehicles Penetration on Electricity Demand, Prices and Thermal Generation Dispatch", International Conference on European Energy Market (EEM), 2012.

[51] A. S. Masoum, S. Deilami, A. Abu-Siada and M. A. S. Masoum, "Fuzzy approach for online coordination of plug-in electric vehicle charging in smart grid", IEEE Transaction on Sustainable Energy, Vol.6, No.3, pp.1112-1121, 2015.

[52] P. Papadopoulos, N. Jenkins, L. M. Cipcigan, I. Grau and E. Zabala, "Coordination of the Charging of Electric Vehicles Using a Multi-agent System", IEEE Transaction on Smart Grid, Vol.4, No.4, pp.1802-1809, 2013.

[53] A. Zakariazadeh, S. Jadid, P. Siano, "Multi-objective scheduling of Electric Vehicles in Smart Distribution System", Energy Conversion and Management, Vol.79, pp.43-53, 2014.

[54] J. Soares, M.A. Fotouhi Ghazvini, M. Silva, Z. Vale, "Multi-dimensional signalling method for Population-based Metaheuristics: Solving the large-Scale Scheduling Problem in Smart Grids", Swarm and Evolutionary Computation, 2016.

[55]Y. Luo, T. Zhu, S. Wan, S. Zhang, K. Li, "Optimal Charging Scheduling for Large-scale EV (Electric Vehicle) Deployment based on the Interaction of the Smart-grid and Intelligent-transport Systems", Energy ,Vol.97, pp.359–368, 2016.

[56] Z. Ma, D. Callaway, I. Hiskens, "Decentralized Charging Control for Large Populations of Plug-in Electric Vehicles: Application of the Nash Certainty Equivalence Principlee", IEEE Conference of Control Application, pp. 191-195, 2010.

[57] S. Hajforoosh, M.A.S. Masoum, S.M. Islam, "Real-time Charging Coordination of Plug-in electric Vehicles based on Hybrid Fuzzy Discrete Particle Swarm Optimization," Electric Power Systems Research," pp.19–29, 2015.

[58] X. Luo, K.W. Chan, "Real time Scheduling of Electric Vehicles Charging in low-voltage Residential distribution Systems to Minimize Power losses and Improve Voltage Profile", IET Proceedings on Generation, Transmission and Distribution, Vol.8, No.3, pp.516-529, 2013.

[59] E. Gerding et al., "Online Mechanism Design for Electric Vehicle Charging," International Conference of Autonomous Multi agent System, pp.811-818, 2011.

[60] Y. He, B. Venkatesh, and L. Guan, "Optimal Scheduling for Charging and Discharging of Electric Vehicles," IEEE Transaction Smart Grid, Vol.3, No.3, pp. 1095–110, 2012.

[61] S. Han, S. Han, K. Sezaki, "Development of an Optimal Vehicle to Grid Aggregator for frequency Regulation", IEEE Transaction on Smart Grid, Vol. 1, No. 1, 2010.

[62] E. Sortomme, M.A. El-Sharkawi, "Optimal Charging Strategies for Unidirectional Vehicle to Grid", IEEE Transaction on Smart Grid, Vol.2, No.1, pp.131-138, 2011.

[63] M. Alonso, H. Amaris, J.G. Germain, J. M. Galan, "Optimal Charging Scheduling of Electric Vehicles in Smart grids by Heuristic Algorithms", Journal of Energies, Vol.7, No.4, 2014.

[64] D.T. Nguyen, L.B. Le, "Joint Optimization of Electric Vehicle and Home Scheduling Considering User Comfort Preference", IEEE Transaction on Smart Grid, Vol.5, No.1, pp.188-199, 2014.

[65] M.H. Amirioun, A. Kazemi, "A New Model based on Optimal Scheduling of Combined Energy Exchange for Aggregation of Electric Vehicles in a Residential Complex", IEEE Journal on Energies, Vol.69, pp.186-198, 2014.

[66] C.T. Li, C. Ahn, H. Peng, J. Sun, "Synergistic Control of Plug-In Vehicle Charging and Wind Power Scheduling", IEEE Transaction on Power Systems, Vol.28, No.2, pp.1113-1121, 2013.

[67] I. Sharma, C. A. Ca˜nizares, K. Bhattacharya, "Modeling and Impacts of Smart Charging PEVs in Residential Distribution Systems," Power and Energy Society General Meeting, pp. 1–8, 2012.

[68] I. Sharma, C. Canizares, B. Bhattacharya, "Smart Charging of PEVs Penetrating into Residential Distribution Systems", IEEE Transaction on Smart Grid, Vol.5, No.3, pp.1196-1209, 2014.

[69] J. Taylor, A. Maitra, M. lexander, D. Brooks, M. Duvall, "Evaluation of the Impact of Plug-in Electric Vehicle Loading on Distribution System Operations", IEEE Power Energy Society General Meeting (PES), pp. 1-6, 2011.

[70] A. Karnama, "Analysis of Integration of Plug-in Hybrid Electric Vehicles in the Distribution Grid", MA Thesis, Royal Institute of Technology (KTH), 2009.

[71] S. Shao, M. Pipattanasomporn, S. Rahman, "Challenges of PHEV Penetration to the Residential Distribution Network", IEEE Power Energy Society General Meeting (PES), pp. 1–8, 2009.

[72] Smith, R., Shahidinejad, S., Blair, D., Bibeau, E. L. "Characterization of Urban Commuter Driving Profiles to Optimize Battery Size in Light-duty Plug-in Electric Vehicles", Transportation Research Part D, Vol. 16 No. 3, pp. 218- 224, 2011.

[73] J.C. Kelly, J.S. Macdonald, G.A. Keoleian, "Time-Dependent Plug-in Hybrid Electric Vehicle Charging Based on National Driving Patterns and Demographics", Applied Energy, Vol. 93, pp. 395- 405, 2012.

[74] A. Bin Humayd and K. Bhattacharya, "Impact of PEV penetration on distribution system planning considering time-of-use electricity prices," PES General Meeting Conference, pp. 1-5, 2014.

[75] S. Hajfroosh, M.A.S. Masoum, S. Islam, "Performance Analysis of Optimal Online and Delayed Charging of Plug-in Electric Vehicles, ELECO Conference, 2015.

[76] S.M.H, Nabavi, A. Kazemi, M.A.S. Masoum, "Social Welfare Improvement by TCSC using Real Code Based Genetic Algorithm in Double-Sided Auction Market," Journal on Scientia Iranica, Vol. 19, No. 3, 2012.

[77] A. D. Rana, J. B. Darji, P. G. Pandya, "Backward / Forward Sweep Load Flow Algorithm for Radial Distribution System", International Journal for Scientific Research & Development, Vol. 2, No.1, pp. 398-400, 2014.

[78] Z. Luo, Z. Hu, Y. Song, Z. Xu, H. Lu, "Optimal Coordination of Plug-in Electric Vehicles in Power Grids with Cost-Benefit Analysis - Part I: Enabling Techniques," IEEE Transaction on Power Systems, Vol. 28, No. 4, pp. 3546-3555, 2013.

[79] K. Valentine, W.G. Temple, K.M. Zhang, "Intelligent Electric Vehicle Charging: Rethinking the Valley-Fill," Journal of Power Sources, Vol.196, No.24, pp. 10717–10726, 2011.

[80] S.Y. Derakhshandeh, A.S. Masoum, S. Deilami, M.A.S. Masoum, M.E.H.Golshan, "Coordination of Generation Scheduling with PEVs Charging in Industrial Microgrids," IEEE Transaction on Power Systems, Vol. 28, No. 3, pp. 3451-3461, 2013.

[81] M.A.S. Masoum, P.S. Moses, S. Hajforoosh, "Distribution Transformer Stress in Smart Grid with Coordinated Charging of Plug-in Electric Vehicles," IEEE Power Energy Soc. Innovative Smart Grid, pp. 1–8, 2012.

[82] P. Richardson, D. Flynn, A. Keane, "Optimal Charging of Electric Vehicles in Low-Voltage Distribution Systems," IEEE Transaction on Power Systems, Vol. 27, No.1, pp. 268-279, 2012.

[83] A.S. Masoum, S. Deilami, P.S. Moses, M.A.S. Masoum, A. Abu-Siada, "Smart Load Management of Plug-in Electric Vehicles in Distribution and Residential Networks with Charging Stations for Peak Shaving and Loss Minimization Considering Voltage Regulation," IET Proceedings on Generation, Transmission and Distribution, Vol. 5, No. 8, pp. 877-888, 2011.

[84] W. Burke, D. Auslander, "Residential Electricity Auction with Uniform Pricing and Cost Constraints," North American Power Symposium, pp. 1-6, 2009.

[85] A. Attanasio, G. Ghiani, L. Grandinetti, F. Guerriero, "Auction Algorithms for Decentralized Parallel Machine Scheduling," Parallel Computing 32, Vol. 32, No. 9, pp. 701-709, 2006.

[86] R.A. Waraich, M.D. Galus, C. Dobler, M. Balmer, G. Andersson, K.W. Axhausen, "Plug-in Hybrid Electric Vehicles and Smart Grids: Investigations Based on a Microsimulation," Transportation Research Part C: Emerging Technologies, Vol. 28, pp. 74-86, 2013.

[87] R. Liu, L. Dow, E. Liu, "A Survey of PEV Impacts on Electric Utilities," IEEE PES ISGT Conference, pp. 1-8, 2011.

[88] T-K. Lee, Z. Baraket, T. Gordon, Z. Filipi, "Stochastic Modeling for Studies of Real-world PHEV Usage: Driving Schedules and Daily Temporal distributions," IEEE Transaction on Vehicular Technology, Vol. 61, No.4, 2012.

[89] J. Kennedy, R.C. Eberhart, "A Discrete Binary Version of Particle Swarm Algorithm," IEEE International Conference on Computational Cybernetics and Simulation, Vol. 5, pp. 4101- 4108, 1997.

[90] S. Hajforoosh, S.M.H. Nabavi, M.A.S. Masoum, "Coordinated Aggregated-based Particle Swarm Optimisation Algorithm for Congestion Management in Restructured Power Market by Placement and Sizing of Unified Power Flow Controller," IET Science Measurement & Technology , Vol.6, No.4, pp. 267-278, 2012.

[91] W. Di, C. Chengrui, D.C. Alprantis, "Potential Impacts of Aggregator-Controlled Plug-in Electric Vehicles on Distribution Systems," IEEE International Conference on Computational Advances, pp. 105-108, 2011.

[92] H. Nordman, M. Lahtinen, "Thermal overload tests on a 400-MVA Power transformer with a Special 2.5-p.u. Short time Loading Capability," IEEE Transaction on Power Delivery, Vol. 18, No.1, pp. 107 – 112, 2003.

[93] S. Dejan, "Dynamic thermal Modelling of Power Transformers", Doctoral Dissertation, TKK Dissertations, 2005.

[94] Transformers Committee of the IEEE Power Engineering Society, IEEE Std C57.91-1995: IEEE Guide for Loading Mineral-Oil-Immersed Transformers, 1995.

[95] http://www.chargepoint.com/evs

[96] Q. Gong, S. Midlam-Mohler, V. Marano, G. Rizzoni, "Study of PEV Charging on Residential Distribution Transformer Life," IEEE Transactions on Smart Grid, Vol.3, No.1, pp. 404-412, 2012.

[97] PSERC Publication 11-02, "Transformer Overloading and Assessment of Loss-of- Life for Liquid-Filled Transformers," pp. 20-37, 2011.

[98] IEC 60076-7, Loading Guide for Oil-immersed Power Transformers, 2005

[99] Wenhua H. Zhu, Ying Zhu, B.J. Tatarchuk, "A Simplified Equivalent Circuit Model for Simulation of Pb–Acid Batteries at Load for Energy Storage Application", Energy Conversion and Management, pp. 2794-2799, 2011.

[100] M.M. Mahmoud, "On the Storage Batteries Used in Solar Electric Power Systems and Development of an Algorithm for Determining their Ampere-hour Capacity, Electric Power Systems Research", Vol. 71, pp. 85-89, 2004.

[101] P. Sabine, P. Marion, J. Andreas, "Methods for State-of-charge Determination and their Applications", Journal of Power Sources, Vol. 96, pp 113-120, 2001.

[102] P.E. Pascoe, A.H. Anbuky, "Estimation of VRLS Battery Capacity using the Analysis of Coup de Fouet Region", Telecommunication Energy Conference (INTELEC), 1999.

[103] C.h. Ehret, S. Piller, W. Schroer, A. Jossen, "State-of-charge Determination for Lead-acid Batteries in PV-applications", European Photovoltaic Solar Energy Conference, pp. 2486-2489, 2000.

[104] S. Hajforoosh, M.A.S. Masoum, S.M. Islam, "Online Optimal Variable Charge-rate Coordination of Plug-In Electric Vehicles to Maximize Customer Satisfaction and Improve Grid Performance", Electric Power Systems Research, pp.407-420, 2016.

[105] https://www.ecnmag.com/article/2012/11/fundamentals-battery-fuelgauging.

Appendix A

Statement of the Co- Authors

Publications:

- S. Hajforoosh, M.A.S. Masoum, S.M. Islam, "Online Optimal Variable Charge-rate Coordination of Plug-In Electric Vehicles to Maximize Customer Satisfaction and Improve Grid Performance", Electric Power Systems Research, pp.407-420, 2016.

- S. Hajforoosh, M.A.S. Masoum, S.M. Islam, "Real-time Charging Coordination of Plug-In Electric Vehicles based on Hybrid Fuzzy Discrete Particle Swarm Optimization", Electric Power Systems Research, pp.19-29, 2015.

- S. Hajforoosh, M.A.S. Masoum, S.M. Islam, "Performance Analysis of Optimal Online and Delayed Charging of Plug-in Electric Vehicles", Conference on Electrical and Electronics Engineering, 2015.

Principal Author (Candidate)

Name of Principal Author	Somayeh Hajforoosh
Contribution to the Papers	- Coordinated the projects. - Developed the theory. - Designed and programmed the models. - Programming and simulation analysis. - Interpretation of the results. - Verified the results and drafted the manuscripts.
Overall Percentage	75%

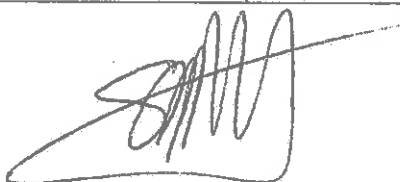Signature: Somayeh Hajforoosh   Date:15/06/2019

Co- Authors Contributions

I, as a Co-Author, endorse that this level of contribution by the candidate indicated above is appropriate.

1- Professor Syed Islam, Project Supervisor

Name of Co-Author	Professor Syed Islam
Contribution to the Papers	• Planned and Supervised the research works • Provided critical feedbacks • Revised the manuscripts
Overall Percentage	12.5%

Signature: Date: 16/6/2019

2- Professor Mohammad Ali Sherkat Masoum, Project Co-Supervisor

Name of Co-Author	Professor Mohammad Ali Sherkat Masoum
Contribution to the Papers	• Planned and Supervised the research works • Provided critical feedbacks • Revised the manuscripts
Overall Percentage	12.5%

Signature: Shkl Masr n12 Date: 17/6, 2019